HHS Public Access

Author manuscript

*J Immunol*. Author manuscript; available in PMC 2022 May 01.

Published in final edited form as:

*J Immunol*. 2021 May 01; 206(9): 2122–2134. doi:10.4049/jimmunol.2100018.

# Prefusion F-based polyanhydride nanovaccine induces both humoral and cell-mediated immunity resulting in long-lasting protection against respiratory syncytial virus

**Laura M. Stephens**[*], **Kathleen A. Ross**[†,‖], **Kody A. Waldstein**[*], **Kevin L. Legge**[*,‡,§,‖], **Jason S. McLellan**[¶], **Balaji Narasimhan**[†,‖], **Steven M. Varga**[*,‡,§,‖]

[*]Interdisciplinary Graduate Program in Immunology, University of Iowa, Iowa City, Iowa, 52242

[†]Department of Chemical and Biological Engineering, Iowa State University, Ames, Iowa, 50011

[‡]Department of Microbiology and Immunology, University of Iowa, Iowa City, Iowa, 52242

[§]Department of Pathology, University of Iowa, Iowa City, Iowa, 52242

[¶]Department of Molecular Biosciences, The University of Texas at Austin, Austin, Texas, 78712

[‖]Nanovaccine Institute, Ames, Iowa, 50011

## Abstract

Respiratory syncytial virus (RSV) is a leading cause of lower respiratory tract infection in both young children and in older adults. Despite the morbidity, mortality, and high economic burden caused by RSV worldwide, no licensed vaccine is currently available. We have developed a novel RSV vaccine composed of a prefusion-stabilized variant of the fusion (F) protein (DS-Cav1) and a CpG oligodeoxynucleotide adjuvant encapsulated within polyanhydride nanoparticles, termed RSVNanoVax. A prime-boost intranasal administration of RSVNanoVax in BALB/c mice significantly ameliorated weight loss and pulmonary dysfunction in response to an RSV challenge, with protection maintained up to at least six months post-vaccination. In addition, vaccinated mice exhibited rapid viral clearance in the lungs as early as two days after RSV infection in both inbred and outbred populations. Vaccination induced an increased number of tissue-resident memory CD4 and CD8 T cells in the lungs, as well as RSV F-directed neutralizing antibodies. Based on the robust immune response elicited and the high level of durable protection observed, our prefusion RSV F nanovaccine is a promising new RSV vaccine candidate.

## Introduction

Respiratory syncytial virus (RSV) is the leading cause of lower respiratory tract infections (LRTI) in children, accounting for nearly 7% of deaths in infants less than one year of age (1, 2). Despite repeated RSV infection throughout an individual's lifespan, natural exposure to the virus generates insufficient and incomplete immunity, particularly in individuals >65 years old (3, 4). This leaves older and immune-suppressed individuals susceptible to severe outcomes including pneumonia and bronchiolitis upon reinfection that results in an

Corresponding Author: Steven M. Varga, Phone Number: 319-335-7784, steven-varga@uiowa.edu.

estimated 14,000 deaths annually in adults over the age of 65 (5, 6). RSV also causes a major economic burden, resulting in more than $300 million in annual medical costs due to hospitalizations in the United States alone (7). There is currently no licensed RSV vaccine. RSV vaccine development has been hampered by prolonged concerns about vaccine safety that arose following the failure of a formalin-inactivated RSV (FI-RSV) vaccine trial in the 1960s (8–11). The inability of the FI-RSV vaccine to elicit a CD8 T cell response combined with the induction of non-neutralizing antibodies and a pathogenic memory CD4 T cell response led to vaccinated children developing enhanced respiratory disease following a natural RSV infection, resulting in the death of two children (12–14). Given the global health and economic burden caused by RSV, there is a critical need for a safe and efficacious vaccine.

The RSV virion consists of three surface proteins: the small hydrophobic (SH) protein, the attachment (G) protein, and the fusion (F) protein (15). Following attachment through the G protein, fusion between the viral envelope and the cell plasma membrane is facilitated by interactions between the F protein and one or more host cell proteins including IGF1R and nucleolin (16, 17). The RSV F protein exists in various configurations, residing in a metastable prefusion structure (preF) prior to fusion, and undergoing a conformation change to a postfusion state (postF) after fusion occurs (18). The preF conformation can be stabilized by the inclusion of two cavity filling mutations and a disulfide bond (DS-Cav1) that prevent structural rearrangements of the protein (19). The preF structure possesses unique antigenic sites, targeted by neutralizing antibodies, that are largely concealed on the postF conformation (20). Previous studies have also demonstrated that DS-Cav1 can elicit robust levels of RSV-neutralizing antibodies (19, 21). Importantly, the majority of neutralizing activity in human serum is attributed to antibodies that target epitopes only exposed on the preF conformation (22, 23). Under certain circumstances such as a soluble F platform or in combination with a Th2-skewing adjuvant, limiting doses of the F protein can elicit non-neutralizing antibodies that contribute to immunopathology (24–27). Importantly, delivery of the F protein in either a particle-based vehicle or inclusion of a TLR agonist can render F-based vaccines safe and effective (24, 28). These studies suggest that the use of a Th1-skewing adjuvant and the selection of vaccine dose are critical factors in designing a vaccine that incorporates the RSV F protein.

Polyanhydride nanoparticles composed of 1,8-bis(*p*-carboxyphenoxy)-3,6-dioxaoctane (CPTEG) and 1,6-bis-(*p*-carboxyphenoxy)hexane (CPH) polymers have been demonstrated to be an effective vaccine platform when delivered either intranasally (i.n.) or subcutaneously (s.c.) (29–31). The hydrophobicity of the particles results in surface erosion, allowing for sustained release of the encapsulated payload and prolonged exposure of the antigen to immune cells (32, 33). The exclusion of water from the particles may also aid in antigen stabilization, by reducing aggregation to maintain native protein structure and function throughout formulation and delivery (34–39). Additionally, the nano-sized particles are an ideal method for inducing protective immunity within the respiratory tract, as nanoscale delivery enhances deposition in the lung and increases uptake into mucosal surfaces (40, 41). Polyanhydrides are also biocompatible and break down in vivo into naturally removed byproducts (42, 43). The particles themselves have been shown to exhibit immunomodulatory properties, such as increasing the activation of antigen presenting cells

(APCs), leading to enhanced adaptive immune responses (44, 45). Finally, i.n. administration of polyanhydride nanoparticles encapsulating bovine RSV (BRSV) antigens to calves showed reduced viral load and pathology in the lungs post-BRSV challenge (46).

In this work, we tested the protective capacity of an i.n. administered CPTEG:CPH-based nanovaccine, termed RSVNanoVax, that encapsulates the RSV preF protein and a CpG 1668 oligodeoxynucleotide adjuvant. Our results demonstrate that a prime-boost immunization with RSVNanoVax provided complete protection from RSV-induced disease and induced rapid clearance of virus from the lungs that was maintained for at least six months post-vaccination. Importantly, viral clearance was also observed in an outbred population. Vaccination induced robust numbers of tissue resident memory ($T_{RM}$) CD4 and CD8 T cells within the lungs, and high titers of F-directed antibodies and serum neutralizing antibodies that were stable out to six months post-vaccination. Altogether, our findings demonstrate that RSVNanoVax is a promising vaccine candidate that generates long-lasting and robust immunity against RSV.

## Materials and Methods

### Mice

Female BALB/c and Swiss Webster mice 6–8 weeks of age were either purchased from the National Cancer Institute/Charles River Laboratories, Inc (Fredrick, MD) or bred at the University of Iowa (Iowa City, IA). All experimental procedures utilizing mice were approved and carried out in accordance with the University of Iowa Animal Care and Use Committee under Animal Protocol #7041999. The experiments were performed under strict accordance to the Office of Laboratory Animal Welfare guidelines and the Public Health Service Policy on Humane Care and Use of Laboratory Animals.

### Nanoparticle synthesis

1,8-bis(*p*-carboxyphenoxy)-3,6-dioxoctane (CPTEG) and 1,6-bis(*p*-carboxyphenoxy)hexane (CPH) monomers were synthesized as previously described (34, 47). 20:80 CPTEG:CPH copolymer was synthesized as previously described (47). 20:80 CPTEG:CPH nanoparticles containing 2% CpG (ODN 1668, Invivogen, San Diego, CA) and/or 1% RSV prefusion F (DS-Cav1, a gift from Dr. Jason McLellan, University of Texas at Austin, Austin, TX) were synthesized via solid-oil-oil double emulsion (43). Briefly, copolymers, RSV F, and CpG were dissolved at a polymer concentration of 20 mg/mL in methylene chloride. The solution was sonicated for 30 s and precipitated into chilled pentane. The resulting nanoparticles were collected via vacuum filtration and their morphology and size were characterized using scanning electron microscopy (FEI Quanta 250, FEI, Hillsboro, OR).

### Prime-boost vaccination

Nanoparticles were suspended in PBS using an ultrasonic water bath (Branson 3510, Danbury, CT). Mice were anesthetized with isoflurane and administered i.n. a dose of 500 μg of nanoparticles. RSVNanoVax contains 5μg preF and 10 μg CpG per dose. CpGNanoVax contains 10 μg CpG per dose. In prime-boost experiments all groups received an identical second dose of the vaccine i.n. on day 28. Control mice, referred to as the no

vaccine group, were administered an equivalent volume of sterile PBS. RSV immune mice received $4.8 \times 10^6$ plaque-forming units (PFU) RSV-A2 on day 0 and a second infection with $4.8 \times 10^6$ PFU RSV-A2 on the date of challenge. For prime only experiments, a single dose of 500 μg nanoparticles was administered, followed by an i.n. RSV challenge on day 28.

### Viruses and infection

The A2 strain of RSV was a gift from Dr. Barney Graham (National Institutes of Health, Bethesda, MD). The line 19 strain was a gift from Dr. Nicholas Lukacs (University of Michigan, Ann Arbor, MI). Both strains were propagated in HEp-2 cells (ATCC, Manassas, VA). Mice were infected i.n. with $1.1 – 4.8 \times 10^6$ PFU RSV while anesthetized with isoflurane.

### Pulmonary function and weight loss

Mice were evaluated daily following RSV infection for weight loss and pulmonary function using a whole-body plethysmograph (Data Sciences International, New Brighton, MN) to measure changes in respiration from baseline measurements taken prior to infection. Enhanced pause (Penh) and mid-tidal expiratory flow (EF50) parameters were calculated based on pressure and volume changes in the chamber caused by respiration and averaged over a 5 min period.

### Plaque assay for viral titers

Whole lungs were harvested, homogenized, and supernatant was flash frozen and stored at −80°C until further use. To measure RSV viral titers, 1:10 dilutions of lung supernatants were added on Vero cells (ATCC) in 6-well plates and mechanically rocked for 90 min at room temperature. Wells were overlaid with 1:1 mixture complete Eagle minimum essential medium (EMEM; Corning, Corning, NY) and 1% SeaKem ME agarose (Cambrex, North Brunswick, NJ). Plates were incubated for five days at 37°C with 5% $CO_2$, then stained with a 1:1 mixture of complete EMEM and 1% agarose containing 0.015% neutral red (Sigma-Aldrich, St. Louis, MO). Viral plaques were counted following an additional 24 h incubation at 37°C and 5% $CO_2$.

### Antibody ELISA

Serum was collected on specified days and RSV F-directed antibody measured by ELISA as previously described (14). For RSV F-directed IgA antibody titers, whole lungs were harvested, homogenized, and supernatant was flash frozen and stored at −80°C until further use. Nasal fluid was collected by cannulation of the trachea and 300 μL of RPMI 1640 (Gibco, Grand Island, NY) was washed through the nasal passage, collected out the nose, and stored at −80°C. Briefly, Nunc MaxiSorp microtiter plates (Thermo Fisher, Rochester, NY) were coated with prefusion RSV F protein (1 μg/mL) or postfusion RSV F protein (1 μg/mL) and incubated overnight at 4°C. Plates were blocked with 5% non-fat dry milk in PBS for one hour at 37°C. Samples were serially diluted 2-fold starting at 1:32 (serum) or 1:1 (lungs and nasal wash) over eight total dilutions and plates were incubated overnight at 4°C. Antibodies specific for RSV F were detected using biotinylated goat anti-mouse

antibody specific for IgG, IgG1, IgG2a, or IgA (Southern Biotech, Birmingham, AL) at a dilution of 1:500. Plates were incubated with a 1:400 dilution of streptavidin-horse radish peroxidase conjugate (Sigma-Aldrich), developed in 3,3',5,5'-tetramethylbenzidine solution (Sigma-Aldrich), and the reaction was stopped with 2 M sulfuric acid. Absorbance values (450nm) were measured and assessed using Gen5 software (BioTek, Winooski, VT).

### Neutralizing antibody titers

Serum was collected on specified days and stored at −80°C until further use. To measure neutralizing antibody titers, serum was first heated at 56°C for 30 min to inactivate complement. Serum samples were diluted 2-fold (1:16 to 1:32768) in a 96-well plate, mixed with 750 PFU RSV-A2, and incubated at 37°C for one hour. 100 μL of virus/serum mixture was added to Vero cells (ATCC) in 12-well plates and mechanically rocked for 90 min at room temperature. Plates were overlaid, incubated, and stained as described above for the viral titer plaque assay. A 4-parameter fit curve analysis was used to determine the serum dilution that resulted in 50% inhibition of RSV viral plaques.

### Competition antibody ELISA

Serum was collected on specified days and stored at −80°C until further use. Motavizumab and D25 (kindly provided by Dr. Jason McLellan) were biotinylated using an EZ-Link Sulfo-NHS-LC-Biotinylation kit (Pierce, Rockford, IL) as per manufacturer's instructions. Immulon 2 HB plates (Thermo Fisher, Rochester, NY) were coated with prefusion RSV F protein (0.5 μg/mL) or postfusion RSV F protein (0.75 μg/mL) and incubated overnight at 4°C. Plates were washed with PBS containing 0.05% Tween-20 (Sigma-Aldrich) in between each step. Plates were blocked with 5% non-fat dry milk in PBS for one hour at 37°C. Samples were serially diluted 2-fold starting at 1:8 over eight total dilutions followed by the addition of 50 μL of biotinylated antibody and incubated together for one hour at 37°C. Plates were then incubated with a 1:500 dilution of streptavidin-horse radish peroxidase conjugate (Sigma-Aldrich), developed in 3,3',5,5'-tetramethylbenzidine solution (Sigma-Aldrich), and the reaction was stopped with 2 M sulfuric acid. Absorbance values (450nm) were measured and assessed using Gen5 software (BioTek, Winooski, VT). Wells containing biotinylated antibody in buffer represent the un-competed positive control. Percent inhibition titers were calculated for each serum dilution using the following formula: $((OD_{D25} - OD_{sample}) / OD_{D25}) * 100$. A 4-parameter fit curve analysis was used to determine the serum dilution that resulted in 50% inhibition of monoclonal antibody binding.

### Antibody staining and flow cytometry

Single-cell suspensions from lungs were prepared as previously described (48, 49). Briefly, lobes were minced and digested in 4 mL of HBSS supplemented with 60 U/mL DNase I (Sigma-Aldrich) and 125 U/mL collagenase (Invitrogen, Carlsbad, CA) for 30 min at 37°C. Digested lungs were pressed through a wire mesh screen (Cellector; Bellco Glass, Inc., Vineland, NJ) to generate a single-cell suspension. Cells were isolated from spleens by gentle dissociation of the organ between frosted microscope slides. For intravascular staining, 1 μg of CD45-APC (30-F11; BioLegend, San Diego, CA) antibody was injected i.v. 3 min prior to euthanasia. Lung cells and splenocytes were stained for extracellular molecules using antibodies for CD90.2 (53–2.1; Thermo Fisher, Waltham, MA), CD4

(RM4–5; BioLegend), CD8 (53–6.7; Thermo Fisher), CD69 (H1.2F3; BioLegend), CD103 (M290; BD Biosciences), CD11a (M17/4; Thermo Fisher), and CD49d (R1–2; BioLegend) for 30 min at 4°C. All cells were fixed with fix/lyse solution (eBioscience) for 10 min at room temperature. For intracellular cytokine staining, cells were stimulated with 50 μg/mL Phorbol 12-myristate 13-acetate (PMA; Sigma-Aldrich) and 500 μg/mL ionomycin (Sigma-Aldrich) for five hours in the presence of 10 μg/mL Brefeldin A (BFA; Sigma-Aldrich). Control wells were stimulated with 10 μg/mL BFA only. Cells were first stained for extracellular molecules, followed by staining with antibodies for IFN-γ (XMG1.2; Thermo Fisher) in 0.5% saponin (Sigma-Aldrich) containing FACS buffer for 30 min at 4°C. For tetramer staining, cells were stained with an optimized concentration of RSV-specific $F_{85–92}$ allophycocyanin-conjugated tetramer for 30 min at 4°C, followed by staining for surface markers as indicated above. Cells were run on an LSRFortessa (BD Biosciences, San Jose, CA) and analyzed using FlowJo software (BD Biosciences). Populations were gated as follows: antigen-experienced CD4 T cells ($CD90.2^+CD4^+CD11a^{hi}CD49d^+$), antigen-experienced CD8 T cells ($CD90.2^+CD8^+CD11a^{hi}CD8^{lo}$), CD4 $T_{RM}$ cells ($CD45^-CD90.2^+CD4^+CD11a^{hi}CD49d^+CD103^-CD69^+$), CD8 $T_{RM}$ cells ($CD45^-CD90.2^+CD8^+CD11a^{hi}CD8^{lo}CD103^+CD69^+$).

## Serum transfer

Serum was collected from the specified group 56 days post-prime vaccination. Prior to euthanasia, blood was collected in heparinized capillary tubes (Fisher Scientific, Pittsburgh, PA) centrifuged at 3000 RPM for 30 min, and serum was collected and frozen at −80°C until further use. Samples were thawed and pooled together per group immediately prior to administration. Recipient mice were administered 200 μL serum/mouse intraperitoneally (i.p.) one day prior to infection.

## RSV fusion protein sequencing

Viral RNA from RSV A2 and line 19 was isolated via standard TRIzol phenol/chloroform extraction (Invitrogen Life Technologies). cDNA was generated using the SuperScript First-Strand Synthesis kit following manufacturer's instructions (Applied Biosystems). Polymerase chain reaction of the RSV fusion protein was performed with 100 ng of template cDNA using the CloneAmp HiFi PCR Premix (Takara Bio USA, Inc., Mountain View, CA) per the manufacturer's instructions with F gene primers 5'Forward-caaacatcataactacactactcac and 5'Reverse-tgaaattcgaggtcattgctt. 0.5 μg of the PCR product and primer 5'Forward-caaaataaactctggggcaaa was subjected to Sanger sequencing by the Genomics Division of the Iowa Institute of Human Genetics.

## Protein modeling

The A2 and line 19 RSV fusion protein amino acid sequences were submitted to the SWISS-model server for 3D structure homology modeling of the RSV fusion protein using known RSV fusion protein structures available on the Research Collaboratory for Structural Bioinformatics Protein Data Bank (RCSB PDB) depository (50–52). The resulting models were visualized and manipulated with ChimeraX version 1.1.1 (53).

### Statistical analysis

All statistical analyses were performed using Prism software (GraphPad Software, Inc., San Diego, CA). Data were evaluated using either one-way ANOVA with Tukey's post hoc test or 2-way ANOVA with Dunnett's post hoc test for comparison between more than two groups. A value of $p<0.05$ was considered significant. Asterisks or pound signs are used to indicate statistical significance between groups as described in each figure legend.

## Results

### Prime-boost vaccination with RSVNanoVax protects against RSV-induced weight loss and pulmonary dysfunction

Efforts to develop a nanoparticle-based RSV vaccine that is administered intramuscularly (i.m.) have recently failed in multiple clinical trials (54). Therefore, we developed an i.n.-delivered vaccine composed of 20:80 CPTEG:CPH nanoparticles encapsulating a stabilized preF construct of the RSV F protein (DS-Cav1) (19). The nanoparticles also contain a B-class CpG 1668 oligodeoxynucleotide adjuvant that functions as a TLR9 agonist to promote cross-presentation by dendritic cells and induce dendritic cell maturation in mice (55, 56). We first asked whether a single i.n. dose of RSVNanoVax would protect against RSV-induced disease. Weight loss and pulmonary function were measured daily as they represent key clinical signatures of disease that are observed following RSV infection in mice (14, 57). Following an RSV challenge at day 28, wild-type (WT) BALB/c mice that received one dose of RSVNanoVax were significantly protected from weight loss compared to mice that received only PBS (No vaccine) (Supplemental Fig. 1A). As an additional control, we vaccinated mice with the same dose of nanoparticles containing only the CpG adjuvant (CpGNanoVax). Mice that received a single dose of CpGNanoVax exhibited weight loss similar to the no vaccine group when challenged with RSV. Next, we used whole-body plethysmography to measure lung function, by tracking the parameters enhanced pause (Penh), an indicator of airway obstruction, and mid-tidal expiratory flow (EF50), a measure of bronchoconstriction (58, 59). Unvaccinated controls or mice that received CpGNanoVax exhibited pulmonary dysfunction, as indicated by an elevation in baseline Penh and EF50, after an acute RSV challenge (Supplemental Fig. 1B, 1C). In contrast, one dose of RSVNanoVax was enough to significantly reduce pulmonary dysfunction compared to controls.

We next asked if greater protection would be afforded by the administration of two doses of RSVNanoVax. All groups received a prime vaccination at day 0 followed by a boost with the same dose on day 28. To match the timeline of the single dose, all groups were challenged 28 days after the last vaccine administration. Mice that received two doses of RSVNanoVax exhibited minimal weight loss (~5%) compared to unvaccinated controls (~25%) following an RSV challenge on day 56 (Fig. 1A). A prime-boost of RSVNanoVax also protected the lungs of vaccinated mice from RSV-induced pulmonary dysfunction (Fig. 1A). To determine the duration of protection afforded by the vaccine, mice were administered a prime-boost vaccination and were challenged with RSV at extended time points. At 100 days post-vaccination, we observed no decrease in the level of protection provided by RSVNanoVax (Fig. 1B). Importantly, mice vaccinated with RSVNanoVax remained protected out to at

least six months post-vaccination (Fig. 1C). Overall, these data demonstrate that a prime-boost vaccination with RSVNanoVax provides long-lasting protection from RSV-induced disease.

## RSVNanoVax vaccinated mice exhibit rapid viral clearance in the lung following RSV challenge

Next, we assessed the ability of a single vaccine dose to promote viral clearance. Unvaccinated controls or WT mice that received CpGNanoVax exhibited high virus titers in their lungs at the peak of RSV replication (on day 4) as determined by plaque assay (Supplemental Fig. 1D) (60). As expected, RSV immune mice exhibited complete protection on day 4 from RSV replication in the lungs upon rechallenge. However, while one dose of RSVNanoVax significantly reduced the amount of virus in the lungs, it failed to induce complete viral clearance. To assess the efficacy of two vaccine doses, prime-boost immunized mice were challenged with RSV on day 56. Similar to the single dose, two doses of CpGNanoVax provided no protection compared to the unvaccinated controls (Fig. 2A). In contrast, prime-boost RSVNanoVax immunization resulted in nearly complete viral clearance in the lungs as early as day 2 (Supplemental Fig. 2), and complete clearance in all mice by day 4 (Fig. 2A). Thus, a prime-boost administration of RSVNanoVax was found to be the most efficacious strategy for inducing complete protection, and was utilized for the remainder of the experiments.

To examine the capacity of RSVNanoVax to promote viral clearance long-term, viral titers were measured in the lungs at multiple time points after vaccination. 100 days post-vaccination, no virus was detectable in 6/9 mice that were immunized with RSVNanoVax (Fig. 2B). A similar level of protection extended out to at least six months post-vaccination (Fig. 2C). Finally, we assessed the capacity of RSVNanoVax to protect against a heterologous strain of RSV. Line 19 is a laboratory RSV strain that induces more severe disease characterized by high levels of IL-13, pulmonary dysfunction, and mucus accumulation in the lungs of mice (61). Prime-boost immunization with RSVNanoVax elicited complete clearance of RSV line 19 compared to unvaccinated controls or CpGNanoVax (Fig. 2D). The RSV F proteins differ by 18 amino acid substitutions between the two virus strains (Supplemental Fig. 3). Overall, vaccination with RSVNanoVax promotes long-lasting protection from viral replication in the lung against both homologous and heterologous RSV strains.

## Prime-boost vaccination with RSVNanoVax elicits high titers of RSV F-directed antibodies

The induction of RSV-specific serum antibodies correlates with reduced disease severity, as infants with mild disease exhibit increased antibody titers compared to those with severe disease (62, 63). Additionally, high serum antibody titers correlate with a reduced risk of secondary exposure (64–67). To investigate the generation of RSV F-directed antibodies, serum was collected from vaccinated WT mice on day 56 or six months post-vaccination. RSVNanoVax generated robust titers of preF-directed IgG and IgG1 in the serum, at levels greater than a single RSV infection (Fig. 3A). Additionally, mice vaccinated with RSVNanoVax displayed higher titers of preF-directed IgG2a compared to RSV immune animals, suggesting the induction of a Th1-like response (68). Serum antibodies directed to

the postF conformation were also assessed and found to be elevated in previously RSV infected animals (Fig. 3B). Similarly, RSVNanoVax induced robust postF-directed IgG, IgG1, and IgG2a titers. Both preF and postF-reactive serum antibody titers were maintained at six months post-RSVNanoVax vaccination (Fig. 3A, 3B). Unsurprisingly, as they contain no RSV antigens, the CpGNanoVax failed to induce either preF- or postF-directed antibodies. Thus, RSVNanoVax induces long-lasting systemic antibodies that are specific for RSV F.

To assess the induction of mucosal antibodies, IgA antibody titers were measured in both the whole lung tissue and in fluid collected via nasal wash. Following a prime-boost RSVNanoVax immunization, preF and postF-directed IgA were detected at high titers in the lung tissue (Fig 3C). The preF-directed IgA titers were greater in vaccinated mice compared to RSV immune animals. In addition, RSVNanoVax induced robust IgA specific for the prefusion conformation in the nasal passages. This suggests that the RSVNanoVax can induce local mucosal antibody responses in both the upper and lower airways.

The RSV F protein contains four major antigenic sites that serve as targets for neutralizing antibody responses. Site Ø is restricted to the preF protein conformation, site I is located only on the postF conformation, and sites II and IV are present on both conformations (69, 70). To determine the site specificity of the serum antibodies generated by RSVNanoVax, competition ELISAs were performed using either D25 or motavizumab to measure binding to either site Ø or site II on the RSV F protein, respectively (18, 71). RSVNanoVax antibodies significantly outcompeted D25 for binding to site Ø on the preF conformation of the F protein (Fig. 4A). The antibodies generated by RSVNanoVax also outcompeted motavizumab for binding to site II on both the preF and postF conformations of the F protein (Fig. 4B, 4C). Serum antibodies from RSV immune animals were unable to outcompete either D25 or motavizumab for binding to the F protein. Naïve mice and CpGNanoVax vaccinated mice exhibited no RSV-specific antibodies to compete with either monoclonal antibody. These data suggest that RSVNanoVax induces antibodies that bind mainly at site Ø on the preF structure, with additional antibodies that bind at site II that is present on both protein conformations.

The preF and postF conformations both possess epitopes commonly targeted by neutralizing antibodies, however, there is evidence that the majority of the neutralizing activity found in human serum comes from antibodies specific to epitopes accessible only on the preF conformation (22, 23). Thus, a vaccine that utilizes the preF protein should induce antibodies with high neutralizing activity. Naïve mice and CpGNanoVax vaccinated mice exhibit no neutralizing antibodies in their serum (Fig. 4D). The preF-specific antibody D25 exhibited high neutralizing activity as expected. Serum antibodies from RSVNanoVax vaccinated mice demonstrated potent neutralizing activity at day 56, with only a small non-significant decline at six months. In comparison, RSV immune serum displayed high titers of RSV neutralizing antibodies at day 56, but exhibited a significant drop in neutralizing titers by six months. Our results indicate that neutralizing RSV-specific antibodies induced by RSVNanoVax are longer lasting compared to antibodies produced by a natural RSV infection.

## RSVNanoVax elicits antigen-experienced tissue-resident memory CD4 and CD8 T cells in the lung

RSV-specific memory T cells play a critical role in limiting disease severity, reducing viral replication, and providing protection against reinfection. In mice, the adoptive transfer of RSV-specific airway CD4 or CD8 T cells that are composed primarily of $T_{RM}$ cells, protects naïve recipients from RSV-induced weight loss (72). Additionally, in humans, airway-localized RSV-specific memory CD8 T cells correlate with reduced symptoms following experimental challenge (73). To examine the capacity of RSVNanoVax to generate RSV-specific memory T cells, lungs were harvested on day 42 from prime-boost vaccinated mice prior to RSV challenge. Surface expression of CD11a and CD49d were utilized as surrogate markers of activation to distinguish antigen-experienced CD4 T cells, along with CD11a and downregulation of CD8α to analyze antigen-experienced CD8 T cells (74, 75). RSVNanoVax elicited a high frequency of antigen-experienced ($CD11a^{hi}CD49d^{+}$) CD4 T cells in the lungs compared to animals that received either PBS or CpGNanoVax (Fig. 5A). The frequency of antigen-experienced ($CD11a^{hi}CD8^{lo}$) CD8 T cells was also increased in the lungs of RSVNanoVax vaccinated mice compared to the controls (Fig. 5B). A similar pattern was observed in the total number of antigen-experienced CD4 and CD8 T cells in the lungs of vaccinated mice (Fig. 5C, 5D). The propensity of RSVNanoVax to elicit antigen-experienced T cells was specific to the lungs, as no increase in the total frequency of antigen-experienced T cells was observed in the spleen of any group (Fig. 5A, 5B). Interestingly, RSVNanoVax generated a higher total number of antigen-experienced CD4 and CD8 T cells compared to an acute RSV infection. Thus, vaccination with RSVNanoVax induced virus-specific memory CD4 and CD8 T cells in the lungs.

Next, we evaluated the capacity of RSVNanoVax to elicit virus-specific $T_{RM}$ T cells, which are key mediators of site-specific protection against respiratory virus reinfections (76, 77). Intravascular staining was utilized to distinguish between cells in the lung tissue from cells transiting within the pulmonary vasculature (78). RSVNanoVax induced a large number of virus-specific memory CD4 and CD8 T cells within the lung tissue expressing CD69 and/or CD103, canonical markers of $T_{RM}$ cells (Fig. 5E, 5F) (79). Of particular note, vaccinated mice had a higher number of $T_{RM}$ CD4 and CD8 T cells compared to both CpGNanoVax and the RSV immune groups, indicating that the vaccine may generate longer-lived memory T cell responses.

We also assessed the specificity and functional capacity of the T cells generated in the lungs by the vaccine. RSVNanoVax induced robust numbers of CD8 T cells specific for the $F_{85–93}$ RSV epitope as measured by tetramer staining (Fig. 6A). Additionally, the majority of these $F_{85–93}$-specific CD8 T cells were localized within the lung tissue as determined by intravascular staining (Fig. 6B). The number of $F_{85–93}$-specific cells was similar between the preF vaccinated mice and those previously exposed to RSV, while CpGNanoVax induced very few RSV F-specific T cells, as would be expected. Using intracellular cytokine staining, CD4 and CD8 T cells in the lungs of RSVNanoVax vaccinated mice also demonstrated a higher capacity to produce IFN-γ compared to controls (Fig. 6C, 6D). Overall, RSVNanoVax induces antigen-experienced memory T cells that are localized

within the lung tissue, specific for the $F_{85–93}$ RSV epitope, and exhibit the capacity to produce IFN-γ upon stimulation.

### Antibodies generated by prime-boost vaccination with RSVNanoVax significantly contribute to protection

To determine the relevant immune cell populations that contribute to protection, serum antibodies from vaccinated mice were transferred one day prior to RSV challenge. Antibodies from previously infected animals provided significant protection from weight loss and pulmonary dysfunction (Fig. 7A–7C). Similarly, the transfer of serum from RSVNanoVax vaccinated mice was sufficient to protect recipients from weight loss and lung dysfunction compared to either naïve or CpGNanoVax serum. A small, but reproducible increase in both Penh and EF50 was detectable around five days post-challenge in groups that received RSVNanoVax serum (Fig. 7B, 7C). Lungs from recipients were also harvested on day 4 post-infection for quantification of viral titers by plaque assay. Groups that received either naïve or CpGNanoVax serum exhibited high viral titers of nearly $10^6$ PFU/g tissue at the peak of viral replication (Fig. 7D). In contrast, serum from animals that previously received either RSVNanoVax or RSV reduced viral replication by approximately 2 logs. However, there remained a detectable level of virus, suggesting that the antibodies generated by RSVNanoVax may not be the only immune component contributing to protection from RSV.

### Prime-boost vaccination with RSVNanoVax provides protection from RSV replication in an outbred population

BALB/c mice are an isogenic model system that allows for highly reproducible studies; however, human populations are genetically diverse. Therefore, it is important to consider the effectiveness of any vaccine candidate in a model with increased genetic variability. We utilized Swiss Webster outbred mice to determine the efficacy of RSVNanoVax in a genetically diverse population (80). Following a prime-boost vaccination, Swiss Webster mice exhibited complete clearance in all mice as early as two days post-RSV infection (Fig. 8). Similarly, animals previously infected with RSV were protected from viral replication on day 2 post-infection. As expected, there was no difference in viral titers between naïve mice and those that received a prime-boost of CpGNanoVax. To assess the generation of RSV F-specific antibodies in an outbred population, serum was collected from vaccinated Swiss Webster mice. RSVNanoVax induced high titers of serum preF-directed total IgG, as well as IgG1 and IgG2a in outbred mice (Fig. 9A). Importantly, the vaccine generated a higher titer of antibodies compared to a single RSV infection. Furthermore, vaccinated mice exhibited high titers of postF-directed IgG and IgG2a (Fig. 9B). Similar to the WT mice, CpGNanoVax failed to induce any RSV F-directed antibodies in outbred animals. Overall, RSVNanoVax mediated rapid viral clearance of an acute RSV infection, and generated robust titers of RSV-specific serum antibodies in an outbred mouse model.

## Discussion

In the present study, we have demonstrated the efficacy of an intranasally delivered polyanhydride nanovaccine for RSV. Because a single dose of RSVNanoVax was unable to

completely eliminate viral infection and replication within the lungs, a prime-boost approach was utilized. Two doses of RSVNanoVax provided complete protection from both RSV-induced weight loss and pulmonary dysfunction, and mediated rapid viral clearance in the lungs as early as day 2 post-RSV infection. In addition, complete protection was observed following a challenge with a heterologous pathogenic RSV strain. Because of the wide genetic diversity present in the human population, it was also important to assess the efficacy of RSVNanoVax in a more diverse outbred population. Swiss Webster mice administered two doses of RSVNanoVax exhibited rapid RSV viral clearance in the lungs as early as day two post-infection. Thus, RSVNanoVax can mediate protection in both WT inbred mice and in more genetically diverse outbred mice. While there are limitations to utilizing mice because they are only semi-permissive to RSV infection, they can still serve as an informative model for translational research. This is supported by the discovery of Palivizumab, which was developed based on findings first demonstrated in the mouse model (81). Thus, while it is important not to over-interpret data from animal models, the manipulability of mice and the wide array of immunological reagents available allows for informative and intricate testing of new vaccine candidates.

RSV infections exhibit seasonality in most geographic locations (82). Thus, an efficacious RSV vaccine should provide protection for at least 4–6 months in order to last through a typical RSV season. Importantly, mice vaccinated with RSVNanoVax remained protected from RSV-induced disease and exhibited nearly complete protection from infectious viral replication in the lungs out to at least six months post-vaccination. Small, but detectable levels of viral replication, were observed in 4/10 mice on day 4 post-infection. Of note, the low levels of virus replication observed in RSVNanoVax vaccinated mice challenged with RSV at day 100 were similar to mice challenged at six months. Thus, the high efficacy of the nanovaccine at day 100 is maintained out to at least six months without a significant decline. To our knowledge, there are very few other RSV nanoparticle-based vaccine candidates that have demonstrated high efficacy at such late time points post-vaccination. In the context of other pathogens including Influenza A virus and *Yersinia pestis*, polyanhydride nanovaccines have induced long-lasting protection 100–280 days post-challenge (29, 83, 84). This demonstrates the potential of this vaccine platform for inducing long term protection.

The majority of current RSV vaccine strategies are focused on inducing neutralizing serum antibodies and/or high titers of mucosal IgA, as they are strong correlates of protection in both infants and adults (62, 63, 67, 85, 86). RSVNanoVax induced high titers of serum antibodies specific for both the preF and postF conformations of the RSV F protein. The antibodies bound strongly to site Ø on the preF structure, as well as site II on both the preF and postF conformations. Antibodies present in the serum of RSVNanoVax vaccinated animals also had a high neutralizing capacity. F-directed antibodies can bind to the F protein prior to infection, interrupting the cell-to-cell fusion process and preventing subsequent viral entry and transcription (87, 88). Additionally, as the infectious RSV virion expresses a combination of preF and postF protein structures on its surface, virus neutralization may be enhanced when antibodies specific for both conformations are present (89). RSVNanoVax also induced high titers of RSV F-directed IgA in both the lung tissue and in the nasal passages. In an adult human experimental RSV challenge model, the ability to successfully

establish an RSV infection inversely correlated with pre-existing virus-specific nasal IgA (85, 90). Of note, the titers of preF-directed serum IgG and lung IgA generated by RSVNanoVax were elevated compared to an acute RSV infection. Thus, RSVNanoVax induced both systemic and local RSV-specific antibody responses.

RSV-specific antibodies have been reported to wane over time, leaving an individual potentially susceptible to re-infection (64, 65, 91, 92). Importantly, we observed no decline in either the preF or postF-directed total IgG or IgG2a antibody titers generated by RSVNanoVax six months post-vaccination. Similarly, no significant decline was observed in the neutralizing capacity of the serum antibodies generated by the nanovaccine out to six months post-vaccination. In contrast, the neutralizing capacity of serum from RSV immune mice significantly declined by six months-post vaccination. This suggests that RSVNanoVax stimulates a longer-lasting humoral immune response compared to a single RSV infection.

Through the adoptive transfer of serum, we demonstrate that serum antibodies generated by RSVNanoVax can provide partial protection from RSV-induced disease. Additionally, the transfer of serum antibodies was able to significantly reduce peak viral titers in the lungs of naïve recipient mice challenged with RSV. However, detectable levels of viral replication were still observed with antibodies alone, suggesting that additional factors may contribute to protection. Thus, RSVNanoVax induced RSV F-directed serum antibodies that maintain long-term neutralizing capacity and contribute to protection from RSV.

While we observed no decline in vaccine-induced serum neutralizing antibody titers, long-term protection from RSV infection would likely be augmented further by the induction of RSV-specific T cells. Neutralizing antibodies predominantly function by reducing the infectivity of virions prior to infection of a host cell, thus virus-specific T cells are required to recognize and eliminate virus-infected cells (93). Virus-specific airway-localized T cells have been shown to play a protective role in reducing the severity of RSV-induced disease and preventing reinfection in animal models (72, 73). In particular, $T_{RM}$ cells serve as the first line of defense from reinfecting respiratory pathogens, making this population an appealing vaccine target (76, 94–96). Only a small number of nanoparticle-based RSV vaccine candidates have assessed the induction of virus-specific T cells, and even fewer have evaluated the $T_{RM}$ phenotype of the cells (97–99). One study demonstrated that i.n. administration of a virus-like particle (VLP) expressing the M and matrix 2 (M2) RSV proteins induced $CD69^{+}CD103^{+}$ CD8 $T_{RM}$ cells in the lungs (100). However, this study was limited in that it failed to assess both the generation of CD4 $T_{RM}$ cells, as well as the induction of antibodies. This may present concerns about safety, as a high number of memory RSV-specific CD8 T cells in the absence of a humoral immune response can lead to immunopathology (101). RSVNanoVax induced robust numbers of RSV-specific memory CD4 and CD8 T cells that expressed canonical markers of $T_{RM}$ cells and were protected from intravascular antibody staining, suggesting that they reside in the lung tissue. Importantly, RSVNanoVax induced an increased number of CD8 $T_{RM}$ cells compared to an acute RSV infection. While the difference was not statistically significant, it supports data from our laboratory showing that RSV-specific resident memory CD8 T cells wane faster than memory CD4 T cells in the lungs (102).

An important distinguishing feature of our nanovaccine is the route of administration. Intranasal vaccination is an attractive delivery method for combating respiratory pathogens, as it allows for the generation of robust mucosal immunity. Lung-localized immunity, characterized by IgA antibody responses and RSV-specific $T_{RM}$ T cell populations, is unlikely to be induced by systemically administered vaccines (72, 103). Thus, i.n. vaccination against respiratory viruses has been shown to be more efficacious than systemic delivery of the same vaccine (103, 104). To date, most RSV nanoparticle-based vaccines have been administered i.m. due to the ease of delivery and lower regulatory hurdles involved in approval (24, 98, 105, 106). ResVax, a polymer nanoparticle core expressing RSV F trimers developed by Novavax has recently been tested in clinical trials as an i.m. vaccine in both older adults and in pregnant females as a maternal immunization (54, 107). Despite demonstrating safety and efficacy in both preclinical and early Phase 1 and 2 clinical trials, the vaccine failed to meet its primary endpoint to reduce the incidence of medically significant RSV-related LRTIs in Phase 3 clinical trials (54, 107, 108). The protection afforded by the vaccine was also short-lived, as demonstrated by a nearly ~50% reduction in the efficacy of ResVax to reduce medically significant RSV-related LRTIs by 180 days post-vaccination. In comparison, RSVNanoVax maintained high neutralizing antibody titers and exhibited minimal reduction in efficacy out to at least 180 days post-vaccination. While airway localized T cell populations were not assessed, systemic administration would likely induce far fewer mucosal $T_{RM}$ T cells compared to our i.n.-delivered RSVNanoVax.

There are a small number of other i.n. RSV nanoparticle vaccines that have been tested in animal models. However, while all of the vaccine modalities induced RSV-specific serum antibodies, several of the candidates failed to mediate complete viral clearance in the lungs (99, 109, 110). Additionally, the duration of protection at late time points post-vaccination was not assessed. The differences in the efficacy between these candidates and RSVNanoVax may be due to either the adjuvant selection or the nanoparticle vehicle itself. The adjuvant can influence the predominant CD4 T cell subset induced during the response. The CpG motifs utilized in our preF nanoparticle vaccine enhance the production of IFN-$\gamma$ and IL-12, promoting a sustained Th1 response that is critical for clearance of RSV (111, 112). This is supported by our findings that RSVNanoVax induced robust numbers of RSV-specific memory T cells in the lung that are capable of producing IFN-$\gamma$. In contrast, aluminum salts such as the aluminum phosphate adjuvant utilized in ResVax can preferentially induce a Th2 response, characterized by production of IL-4 and IgG1 antibodies (113, 114). Our nanovaccine formulation also offers the benefit of co-delivering the antigen and the adjuvant to the same cell, allowing the vaccine to facilitate the induction of a Th1 T cell response in the lungs. Finally, the polyanhydride nanoparticles themselves can function as an adjuvant (83, 115). Dendritic cells cultured with CPTEG:CPH nanoparticles exhibited enhanced expression of MHC II and CD86 compared to untreated cells, resulting in increased antigen-specific CD8 T cell proliferation (44). Thus, our polyanhydride-based formulation containing a CpG adjuvant is formulated to induce a Th1-driven immune response that can provide optimal long-term protection against RSV.

Overall, our data demonstrate that prime-boost immunization with RSVNanoVax induces robust local and systemic RSV-specific antibody responses with high neutralizing capability.

Additionally, RSVNanoVax generates lung tissue-resident memory CD4 and CD8 T cells. Vaccination provides long-lasting protection from RSV-induced disease, and enhances viral clearance in the lungs of both inbred and outbred populations. Altogether, these findings highlight the utility of our unique nanovaccine formulation to induce immunity within the respiratory tract, and provide protection against RSV.

## Supplementary Material

Refer to Web version on PubMed Central for supplementary material.

## Acknowledgements

We wish to thank Stacey Hartwig for all of her technical assistance.

Research reported in this publication was supported by funds from the Iowa State University Nanovaccine Institute (to SMV) and the National Institute of Allergy and Infectious Diseases of the National Institutes of Health under award numbers R01AI124093 (to SMV), T32AI007485 (to LMS), and T32CA078586 (to LMS). The content is solely the responsibility of the authors and does not necessarily represent the official views of the National Institutes of Health.

## References

1. Nair H, Nokes DJ, Gessner BD, Dherani M, Madhi SA, Singleton RJ, O'Brien KL, Roca A, Wright PF, Bruce N, Chandran A, Theodoratou E, Sutanto A, Sedyaningsih ER, Ngama M, Munywoki PK, Kartasasmita C, Simoes EA, Rudan I, Weber MW, and Campbell H. 2010. Global burden of acute lower respiratory infections due to respiratory syncytial virus in young children: a systematic review and meta-analysis. Lancet 375: 1545–1555. [PubMed: 20399493]
2. Scheltema NM, Gentile A, Lucion F, Nokes DJ, Munywoki PK, Madhi SA, Groome MJ, Cohen C, Moyes J, Thorburn K, Thamthitiwat S, Oshitani H, Lupisan SP, Gordon A, Sanchez JF, O'Brien KL, Group PS, Gessner BD, Sutanto A, Mejias A, Ramilo O, Khuri-Bulos N, Halasa N, de-Paris F, Pires MR, Spaeder MC, Paes BA, Simoes EAF, Leung TF, da Costa Oliveira MT, de Freitas Lazaro Emediato CC, Bassat Q, Butt W, Chi H, Aamir UB, Ali A, Lucero MG, Fasce RA, Lopez O, Rath BA, Polack FP, Papenburg J, Roglic S, Ito H, Goka EA, Grobbee DE, Nair H, and Bont LJ. 2017. Global respiratory syncytial virus-associated mortality in young children (RSV GOLD): a retrospective case series. Lancet Glob. Health 5: e984–e991. [PubMed: 28911764]
3. Hall CB, Walsh EE, Long CE, and Schnabel KC. 1991. Immunity to and frequency of reinfection with respiratory syncytial virus. J. Infect. Dis 163: 693–698. [PubMed: 2010624]
4. Henderson FW, Collier AM, Clyde WA Jr., and Denny FW. 1979. Respiratory-syncytial-virus infections, reinfections and immunity. A prospective, longitudinal study in young children. N. Engl. J. Med 300: 530–534. [PubMed: 763253]
5. Falsey AR, Hennessey PA, Formica MA, Cox C, and Walsh EE. 2005. Respiratory syncytial virus infection in elderly and high-risk adults. N. Engl. J. Med 352: 1749–1759. [PubMed: 15858184]
6. Sommer C, Resch B, and Simoes EA. 2011. Risk factors for severe respiratory syncytial virus lower respiratory tract infection. Open Microbiol. J 5: 144–154. [PubMed: 22262987]
7. Paramore LC, Ciuryla V, Ciesla G, and Liu L. 2004. Economic impact of respiratory syncytial virus-related illness in the US: an analysis of national databases. Pharmacoeconomics 22: 275–284. [PubMed: 15061677]
8. Kim HW, Canchola JG, Brandt CD, Pyles G, Chanock RM, Jensen K, and Parrott RH. 1969. Respiratory syncytial virus disease in infants despite prior administration of antigenic inactivated vaccine. Am. J. Epidemiol 89: 422–434. [PubMed: 4305198]
9. Fulginiti VA, Eller JJ, Sieber OF, Joyner JW, Minamitani M, and Meiklejohn G. 1969. Respiratory virus immunization. I. A field trial of two inactivated respiratory virus vaccines; an aqueous trivalent parainfluenza virus vaccine and an alum-precipitated respiratory syncytial virus vaccine. Am. J. Epidemiol 89: 435–448. [PubMed: 4305199]

10. Kapikian AZ, Mitchell RH, Chanock RM, Shvedoff RA, and Stewart CE. 1969. An epidemiologic study of altered clinical reactivity to respiratory syncytial (RS) virus infection in children previously vaccinated with an inactivated RS virus vaccine. Am. J. Epidemiol 89: 405–421. [PubMed: 4305197]

11. Chin J, Magoffin RL, Shearer LA, Schieble JH, and Lennette EH. 1969. Field evaluation of a respiratory syncytial virus vaccine and a trivalent parainfluenza virus vaccine in a pediatric population. Am. J. Epidemiol 89: 449–463. [PubMed: 4305200]

12. Waris ME, Tsou C, Erdman DD, Zaki SR, and Anderson LJ. 1996. Respiratory synctial virus infection in BALB/c mice previously immunized with formalin-inactivated virus induces enhanced pulmonary inflammatory response with a predominant Th2-like cytokine pattern. J. Virol 70: 2852–2860. [PubMed: 8627759]

13. Murphy BR, and Walsh EE. 1988. Formalin-inactivated respiratory syncytial virus vaccine induces antibodies to the fusion glycoprotein that are deficient in fusion-inhibiting activity. J. Clin. Microbiol 26: 1595–1597. [PubMed: 2459154]

14. Knudson CJ, Hartwig SM, Meyerholz DK, and Varga SM. 2015. RSV vaccine-enhanced disease is orchestrated by the combined actions of distinct CD4 T cell subsets. PLoS Pathog. 11: e1004757. [PubMed: 25769044]

15. Tan L, Coenjaerts FE, Houspie L, Viveen MC, van Bleek GM, Wiertz EJ, Martin DP, and Lemey P. 2013. The comparative genomics of human respiratory syncytial virus subgroups A and B: genetic variability and molecular evolutionary dynamics. J. Virol 87: 8213–8226. [PubMed: 23698290]

16. Tayyari F, Marchant D, Moraes TJ, Duan W, Mastrangelo P, and Hegele RG. 2011. Identification of nucleolin as a cellular receptor for human respiratory syncytial virus. Nat. Med 17: 1132–1135. [PubMed: 21841784]

17. Griffiths CD, Bilawchuk LM, McDonough JE, Jamieson KC, Elawar F, Cen Y, Duan W, Lin C, Song H, Casanova JL, Ogg S, Jensen LD, Thienpont B, Kumar A, Hobman TC, Proud D, Moraes TJ, and Marchant DJ. 2020. IGF1R is an entry receptor for respiratory syncytial virus. Nature 583: 615–619. [PubMed: 32494007]

18. McLellan JS, Chen M, Leung S, Graepel KW, Du X, Yang Y, Zhou T, Baxa U, Yasuda E, Beaumont T, Kumar A, Modjarrad K, Zheng Z, Zhao M, Xia N, Kwong PD, and Graham BS. 2013. Structure of RSV fusion glycoprotein trimer bound to a prefusion-specific neutralizing antibody. Science 340: 1113–1117. [PubMed: 23618766]

19. McLellan JS, Chen M, Joyce MG, Sastry M, Stewart-Jones GB, Yang Y, Zhang B, Chen L, Srivatsan S, Zheng A, Zhou T, Graepel KW, Kumar A, Moin S, Boyington JC, Chuang GY, Soto C, Baxa U, Bakker AQ, Spits H, Beaumont T, Zheng Z, Xia N, Ko SY, Todd JP, Rao S, Graham BS, and Kwong PD. 2013. Structure-based design of a fusion glycoprotein vaccine for respiratory syncytial virus. Science 342: 592–598. [PubMed: 24179220]

20. Graham BS, Modjarrad K, and McLellan JS. 2015. Novel antigens for RSV vaccines. Curr. Opin. Immunol 35: 30–38. [PubMed: 26070108]

21. Sastry M, Zhang B, Chen M, Joyce MG, Kong WP, Chuang GY, Ko K, Kumar A, Silacci C, Thom M, Salazar AM, Corti D, Lanzavecchia A, Taylor G, Mascola JR, Graham BS, and Kwong PD. 2017. Adjuvants and the vaccine response to the DS-Cav1-stabilized fusion glycoprotein of respiratory syncytial virus. PLoS One 12: e0186854. [PubMed: 29073183]

22. Ngwuta JO, Chen M, Modjarrad K, Joyce MG, Kanekiyo M, Kumar A, Yassine HM, Moin SM, Killikelly AM, Chuang GY, Druz A, Georgiev IS, Rundlet EJ, Sastry M, Stewart-Jones GB, Yang Y, Zhang B, Nason MC, Capella C, Peeples ME, Ledgerwood JE, McLellan JS, Kwong PD, and Graham BS. 2015. Prefusion F-specific antibodies determine the magnitude of RSV neutralizing activity in human sera. Sci. Transl. Med 7: 309ra162.

23. Magro M, Mas V, Chappell K, Vazquez M, Cano O, Luque D, Terron MC, Melero JA, and Palomo C. 2012. Neutralizing antibodies against the preactive form of respiratory syncytial virus fusion protein offer unique possibilities for clinical intervention. Proc. Natl. Acad. Sci. USA 109: 3089–3094. [PubMed: 22323598]

24. Lee Y, Lee YT, Ko EJ, Kim KH, Hwang HS, Park S, Kwon YM, and Kang SM. 2017. Soluble F proteins exacerbate pulmonary histopathology after vaccination upon respiratory syncytial virus challenge but not when presented on virus-like particles. Hum. Vaccin. Immunother 13: 2594–2605. [PubMed: 28854003]

25. Schneider-Ohrum K, Bennett AS, Rajani GM, Hostetler L, Maynard SK, Lazzaro M, Cheng LI, O'Day T, and Cayatte C. 2019. CD4(+) T cells drive lung disease enhancement induced by immunization with suboptimal doses of RSV fusion protein in the mouse model. J. Virol 93: e00695–19. [PubMed: 31092578]
26. Eichinger KM, Kosanovich JL, Gidwani SV, Zomback A, Lipp MA, Perkins TN, Oury TD, Petrovsky N, Marshall CP, Yondola MA, and Empey KM. 2020. Prefusion RSV F immunization elicits Th2-mediated lung pathology in mice when formulated with a Th2 (but not a Th1/Th2-balanced) adjuvant despite complete viral protection. Front. Immunol 11: 1673. [PubMed: 32849580]
27. Schneider-Ohrum K, Cayatte C, Bennett AS, Rajani GM, McTamney P, Nacel K, Hostetler L, Cheng L, Ren K, O'Day T, Prince GA, and McCarthy MP. 2017. Immunization with low doses of recombinant postfusion or prefusion respiratory syncytial virus F primes for vaccine-enhanced disease in the cotton rat model independently of the presence of a Th1-biasing (GLA-SE) or Th2-biasing (alum) adjuvant. J. Virol 91: e02180–16. [PubMed: 28148790]
28. Delgado MF, Coviello S, Monsalvo AC, Melendi GA, Hernandez JZ, Batalle JP, Diaz L, Trento A, Chang HY, Mitzner W, Ravetch J, Melero JA, Irusta PM, and Polack FP. 2009. Lack of antibody affinity maturation due to poor Toll-like receptor stimulation leads to enhanced respiratory syncytial virus disease. Nat. Med 15: 34–41. [PubMed: 19079256]
29. Zacharias ZR, Ross KA, Hornick EE, Goodman JT, Narasimhan B, Waldschmidt TJ, and Legge KL. 2018. Polyanhydride nanovaccine induces robust pulmonary B and T cell immunity and confers protection against homologous and heterologous influenza A virus infections. Front. Immunol 9: 1953. [PubMed: 30233573]
30. Vela Ramirez JE, Tygrett LT, Hao J, Habte HH, Cho MW, Greenspan NS, Waldschmidt TJ, and Narasimhan B. 2016. Polyanhydride nanovaccines induce germinal center B cell formation and sustained serum antibody responses. J. Biomed. Nanotechnol 12: 1303–1311. [PubMed: 27319223]
31. Ross K, Senapati S, Alley J, Darling R, Goodman J, Jefferson M, Uz M, Guo B, Yoon KJ, Verhoeven D, Kohut M, Mallapragada S, Wannemuehler M, and Narasimhan B. 2019. Single dose combination nanovaccine provides protection against influenza A virus in young and aged mice. Biomater. Sci 7: 809–821. [PubMed: 30663733]
32. Determan AS, Graham JR, Pfeiffer KA, and Narasimhan B. 2006. The role of microsphere fabrication methods on the stability and release kinetics of ovalbumin encapsulated in polyanhydride microspheres. J. Microencapsul 23: 832–843. [PubMed: 17390625]
33. Haughney SL, Ross KA, Boggiatto PM, Wannemuehler MJ, and Narasimhan B. 2014. Effect of nanovaccine chemistry on humoral immune response kinetics and maturation. Nanoscale 6: 13770–13778. [PubMed: 25285425]
34. Kipper MJ, Wilson JH, Wannemuehler MJ, and Narasimhan B. 2006. Single dose vaccine based on biodegradable polyanhydride microspheres can modulate immune response mechanism. J. Biomed. Mater. Res. A 76: 798–810. [PubMed: 16345084]
35. Schwendeman SP, Costantino HR, Gupta RK, Siber GR, Klibanov AM, and Langer R. 1995. Stabilization of tetanus and diphtheria toxoids against moisture-induced aggregation. Proc. Natl. Acad. Sci. USA 92: 11234–11238. [PubMed: 7479971]
36. Ross KA, Loyd H, Wu W, Huntimer L, Wannemuehler MJ, Carpenter S, and Narasimhan B. 2014. Structural and antigenic stability of H5N1 hemagglutinin trimer upon release from polyanhydride nanoparticles. J. Biomed. Mater. Res. A 102: 4161–4168. [PubMed: 24443139]
37. Haughney SL, Petersen LK, Schoofs AD, Ramer-Tait AE, King JD, Briles DE, Wannemuehler MJ, and Narasimhan B. 2013. Retention of structure, antigenicity, and biological function of pneumococcal surface protein A (PspA) released from polyanhydride nanoparticles. Acta Biomater. 9: 8262–8271. [PubMed: 23774257]
38. Carrillo-Conde B, Schiltz E, Yu J, Chris Minion F, Phillips GJ, Wannemuehler MJ, and Narasimhan B. 2010. Encapsulation into amphiphilic polyanhydride microparticles stabilizes Yersinia pestis antigens. Acta Biomater. 6: 3110–3119. [PubMed: 20123135]
39. Petersen LK, Phanse Y, Ramer-Tait AE, Wannemuehler MJ, and Narasimhan B. 2012. Amphiphilic polyanhydride nanoparticles stabilize Bacillus anthracis protective antigen. Mol. Pharm 9: 874–882. [PubMed: 22380593]

40. Illum L 2007. Nanoparticulate systems for nasal delivery of drugs: a real improvement over simple systems? J. Pharm. Sci 96: 473–483. [PubMed: 17117404]
41. Jakobsson JKF, Aaltonen HL, Nicklasson H, Gudmundsson A, Rissler J, Wollmer P, and Londahl J. 2018. Altered deposition of inhaled nanoparticles in subjects with chronic obstructive pulmonary disease. BMC Pulm. Med 18: 129. [PubMed: 30081885]
42. Gentile P, Chiono V, Carmagnola I, and Hatton PV. 2014. An overview of poly(lactic-co-glycolic) acid (PLGA)-based biomaterials for bone tissue engineering. Int. J. Mol. Sci 15: 3640–3659. [PubMed: 24590126]
43. Ulery BD, Phanse Y, Sinha A, Wannemuehler MJ, Narasimhan B, and Bellaire BH. 2009. Polymer chemistry influences monocytic uptake of polyanhydride nanospheres. Pharm. Res 26: 683–690. [PubMed: 18987960]
44. Torres MP, Wilson-Welder JH, Lopac SK, Phanse Y, Carrillo-Conde B, Ramer-Tait AE, Bellaire BH, Wannemuehler MJ, and Narasimhan B. 2011. Polyanhydride microparticles enhance dendritic cell antigen presentation and activation. Acta Biomater. 7: 2857–2864. [PubMed: 21439412]
45. Jain S, Yap WT, and Irvine DJ. 2005. Synthesis of protein-loaded hydrogel particles in an aqueous two-phase system for coincident antigen and CpG oligonucleotide delivery to antigen-presenting cells. Biomacromolecules 6: 2590–2600. [PubMed: 16153096]
46. McGill JL, Kelly SM, Kumar P, Speckhart S, Haughney SL, Henningson J, Narasimhan B, and Sacco RE. 2018. Efficacy of mucosal polyanhydride nanovaccine against respiratory syncytial virus infection in the neonatal calf. Sci. Rep 8: 3021. [PubMed: 29445124]
47. Torres MP, Vogel BM, Narasimhan B, and Mallapragada SK. 2006. Synthesis and characterization of novel polyanhydrides with tailored erosion mechanisms. J. Biomed. Mater. Res. A 76: 102–110. [PubMed: 16138330]
48. Fulton RB, Meyerholz DK, and Varga SM. 2010. Foxp3+ CD4 regulatory T cells limit pulmonary immunopathology by modulating the CD8 T cell response during respiratory syncytial virus infection. J. Immunol 185: 2382–2392. [PubMed: 20639494]
49. Christiaansen AF, Knudson CJ, Weiss KA, and Varga SM. 2014. The CD4 T cell response to respiratory syncytial virus infection. Immunol. Res 59: 109–117. [PubMed: 24838148]
50. Schwede T, Kopp J, Guex N, and Peitsch MC. 2003. SWISS-MODEL: An automated protein homology-modeling server. Nucleic Acids Res. 31: 3381–3385. [PubMed: 12824332]
51. Waterhouse A, Bertoni M, Bienert S, Studer G, Tauriello G, Gumienny R, Heer FT, de Beer TAP, Rempfer C, Bordoli L, Lepore R, and Schwede T. 2018. SWISS-MODEL: homology modelling of protein structures and complexes. Nucleic Acids Res. 46: W296–W303. [PubMed: 29788355]
52. Berman HM, Westbrook J, Feng Z, Gilliland G, Bhat TN, Weissig H, Shindyalov IN, and Bourne PE. 2000. The Protein Data Bank. Nucleic Acids Res. 28: 235–242. [PubMed: 10592235]
53. Goddard TD, Huang CC, Meng EC, Pettersen EF, Couch GS, Morris JH, and Ferrin TE. 2018. UCSF ChimeraX: Meeting modern challenges in visualization and analysis. Protein Sci. 27: 14–25. [PubMed: 28710774]
54. Madhi SA, Polack FP, Piedra PA, Munoz FM, Trenholme AA, Simoes EAF, Swamy GK, Agrawal S, Ahmed K, August A, Baqui AH, Calvert A, Chen J, Cho I, Cotton MF, Cutland CL, Englund JA, Fix A, Gonik B, Hammitt L, Heath PT, de Jesus JN, Jones CE, Khalil A, Kimberlin DW, Libster R, Llapur CJ, Lucero M, Perez Marc G, Marshall HS, Masenya MS, Martinon-Torres F, Meece JK, Nolan TM, Osman A, Perrett KP, Plested JS, Richmond PC, Snape MD, Shakib JH, Shinde V, Stoney T, Thomas DN, Tita AT, Varner MW, Vatish M, Vrbicky K, Wen J, Zaman K, Zar HJ, Glenn GM, Fries LF, and G. Prepare Study. 2020. Respiratory syncytial virus vaccination during pregnancy and effects in infants. N. Engl. J. Med 383: 426–439. [PubMed: 32726529]
55. Jiang H, Wang Q, Li L, Zeng Q, Li H, Gong T, Zhang Z, and Sun X. 2018. Turning the old adjuvant from gel to nanoparticles to amplify CD8(+) T cell responses. Adv. Sci. (Weinh) 5: 1700426. [PubMed: 29375970]
56. Nierkens S, den Brok MH, Garcia Z, Togher S, Wagenaars J, Wassink M, Boon L, Ruers TJ, Figdor CG, Schoenberger SP, Adema GJ, and Janssen EM. 2011. Immune adjuvant efficacy of CpG oligonucleotide in cancer treatment is founded specifically upon TLR9 function in plasmacytoid dendritic cells. Cancer Res. 71: 6428–6437. [PubMed: 21788345]

57. van Schaik SM, Enhorning G, Vargas I, and Welliver RC. 1998. Respiratory syncytial virus affects pulmonary function in BALB/c mice. J. Infect. Dis 177: 269–276. [PubMed: 9466511]
58. Glaab T, Ziegert M, Baelder R, Korolewitz R, Braun A, Hohlfeld JM, Mitzner W, Krug N, and Hoymann HG. 2005. Invasive versus noninvasive measurement of allergic and cholinergic airway responsiveness in mice. Respir. Res 6: 139. [PubMed: 16309547]
59. Huck B, Neumann-Haefelin D, Schmitt-Graeff A, Weckmann M, Mattes J, Ehl S, and Falcone V. 2007. Human metapneumovirus induces more severe disease and stronger innate immune response in BALB/c mice as compared with respiratory syncytial virus. Respir. Res 8: 6. [PubMed: 17257445]
60. Crowe JE Jr., Murphy BR, Chanock RM, Williamson RA, Barbas CF 3rd, and Burton DR. 1994. Recombinant human respiratory syncytial virus (RSV) monoclonal antibody Fab is effective therapeutically when introduced directly into the lungs of RSV-infected mice. Proc. Natl. Acad. Sci. USA 91: 1386–1390. [PubMed: 8108420]
61. Stokes KL, Chi MH, Sakamoto K, Newcomb DC, Currier MG, Huckabee MM, Lee S, Goleniewska K, Pretto C, Williams JV, Hotard A, Sherrill TP, Peebles RS Jr., and Moore ML. 2011. Differential pathogenesis of respiratory syncytial virus clinical isolates in BALB/c mice. J. Virol 85: 5782–5793. [PubMed: 21471228]
62. Capella C, Chaiwatpongsakorn S, Gorrell E, Risch ZA, Ye F, Mertz SE, Johnson SM, Moore-Clingenpeel M, Ramilo O, Mejias A, and Peeples ME. 2017. Prefusion F, postfusion F, G antibodies, and disease severity in infants and young children with acute respiratory syncytial virus infection. J. Infect. Dis 216: 1398–1406. [PubMed: 29029312]
63. Piedra PA, Jewell AM, Cron SG, Atmar RL, and Glezen WP. 2003. Correlates of immunity to respiratory syncytial virus (RSV) associated-hospitalization: establishment of minimum protective threshold levels of serum neutralizing antibodies. Vaccine 21: 3479–3482. [PubMed: 12850364]
64. Falsey AR, Singh HK, and Walsh EE. 2006. Serum antibody decay in adults following natural respiratory syncytial virus infection. J. Med. Virol 78: 1493–1497. [PubMed: 16998887]
65. Falsey AR, and Walsh EE. 1998. Relationship of serum antibody to risk of respiratory syncytial virus infection in elderly adults. J. Infect. Dis 177: 463–466. [PubMed: 9466538]
66. Lee FE, Walsh EE, Falsey AR, Betts RF, and Treanor JJ. 2004. Experimental infection of humans with A2 respiratory syncytial virus. Antiviral Res. 63: 191–196. [PubMed: 15451187]
67. Luchsinger V, Piedra PA, Ruiz M, Zunino E, Martinez MA, Machado C, Fasce R, Ulloa MT, Fink MC, Lara P, and Avendano LF. 2012. Role of neutralizing antibodies in adults with community-acquired pneumonia by respiratory syncytial virus. Clin. Infect. Dis 54: 905–912. [PubMed: 22238168]
68. Germann T, Bongartz M, Dlugonska H, Hess H, Schmitt E, Kolbe L, Kolsch E, Podlaski FJ, Gately MK, and Rude E. 1995. Interleukin-12 profoundly up-regulates the synthesis of antigen-specific complement-fixing IgG2a, IgG2b and IgG3 antibody subclasses in vivo. Eur. J. Immunol 25: 823–829. [PubMed: 7705414]
69. McLellan JS 2015. Neutralizing epitopes on the respiratory syncytial virus fusion glycoprotein. Curr. Opin. Virol 11: 70–75. [PubMed: 25819327]
70. Rossey I, McLellan JS, Saelens X, and Schepens B. 2018. Clinical Potential of prefusion RSV F-specific antibodies. Trends Microbiol. 26: 209–219. [PubMed: 29054341]
71. Wu H, Pfarr DS, Johnson S, Brewah YA, Woods RM, Patel NK, White WI, Young JF, and Kiener PA. 2007. Development of motavizumab, an ultra-potent antibody for the prevention of respiratory syncytial virus infection in the upper and lower respiratory tract. J. Mol. Biol 368: 652–665. [PubMed: 17362988]
72. Kinnear E, Lambert L, McDonald JU, Cheeseman HM, Caproni LJ, and Tregoning JS. 2018. Airway T cells protect against RSV infection in the absence of antibody. Mucosal Immunol. 11: 249–256. [PubMed: 28537249]
73. Jozwik A, Habibi MS, Paras A, Zhu J, Guvenel A, Dhariwal J, Almond M, Wong EH, Sykes A, Maybeno M, Del Rosario J, Trujillo-Torralbo MB, Mallia P, Sidney J, Peters B, Kon OM, Sette A, Johnston SL, Openshaw PJ, and Chiu C. 2015. RSV-specific airway resident memory CD8+ T cells and differential disease severity after experimental human infection. Nat. Commun 6: 10224. [PubMed: 26687547]

74. McDermott DS, and Varga SM. 2011. Quantifying antigen-specific CD4 T cells during a viral infection: CD4 T cell responses are larger than we think. J. Immunol 187: 5568–5576. [PubMed: 22043009]

75. Rai D, Pham NL, Harty JT, and Badovinac VP. 2009. Tracking the total CD8 T cell response to infection reveals substantial discordance in magnitude and kinetics between inbred and outbred hosts. J. Immunol 183: 7672–7681. [PubMed: 19933864]

76. Wu T, Hu Y, Lee YT, Bouchard KR, Benechet A, Khanna K, and Cauley LS. 2014. Lung-resident memory CD8 T cells (TRM) are indispensable for optimal cross-protection against pulmonary virus infection. J. Leukoc. Biol 95: 215–224. [PubMed: 24006506]

77. Teijaro JR, Turner D, Pham Q, Wherry EJ, Lefrancois L, and Farber DL. 2011. Cutting edge: Tissue-retentive lung memory CD4 T cells mediate optimal protection to respiratory virus infection. J. Immunol 187: 5510–5514. [PubMed: 22058417]

78. Anderson KG, Sung H, Skon CN, Lefrancois L, Deisinger A, Vezys V, and Masopust D. 2012. Cutting edge: intravascular staining redefines lung CD8 T cell responses. J. Immunol 189: 2702–2706. [PubMed: 22896631]

79. Turner DL, Bickham KL, Thome JJ, Kim CY, D'Ovidio F, Wherry EJ, and Farber DL. 2014. Lung niches for the generation and maintenance of tissue-resident memory T cells. Mucosal Immunol. 7: 501–510. [PubMed: 24064670]

80. Tuttle AH, Philip VM, Chesler EJ, and Mogil JS. 2018. Comparing phenotypic variation between inbred and outbred mice. Nat. Methods 15: 994–996. [PubMed: 30504873]

81. Tempest PR, Bremner P, Lambert M, Taylor G, Furze JM, Carr FJ, and Harris WJ. 1991. Reshaping a human monoclonal antibody to inhibit human respiratory syncytial virus infection in vivo. Biotechnology (N Y) 9: 266–271. [PubMed: 1367535]

82. Obando-Pacheco P, Justicia-Grande AJ, Rivero-Calle I, Rodriguez-Tenreiro C, Sly P, Ramilo O, Mejias A, Baraldi E, Papadopoulos NG, Nair H, Nunes MC, Kragten-Tabatabaie L, Heikkinen T, Greenough A, Stein RT, Manzoni P, Bont L, and Martinon-Torres F. 2018. Respiratory syncytial virus seasonality: A global overview. J. Infect. Dis 217: 1356–1364. [PubMed: 29390105]

83. Ulery BD, Petersen LK, Phanse Y, Kong CS, Broderick SR, Kumar D, Ramer-Tait AE, Carrillo-Conde B, Rajan K, Wannemuehler MJ, Bellaire BH, Metzger DW, and Narasimhan B. 2011. Rational design of pathogen-mimicking amphiphilic materials as nanoadjuvants. Sci. Rep 1: 198. [PubMed: 22355713]

84. Ulery BD, Kumar D, Ramer-Tait AE, Metzger DW, Wannemuehler MJ, and Narasimhan B. 2011. Design of a protective single-dose intranasal nanoparticle-based vaccine platform for respiratory infectious diseases. PLoS One 6: e17642. [PubMed: 21408610]

85. Bagga B, Cehelsky JE, Vaishnaw A, Wilkinson T, Meyers R, Harrison LM, Roddam PL, Walsh EE, and DeVincenzo JP. 2015. Effect of preexisting serum and mucosal antibody on experimental respiratory syncytial virus (RSV) challenge and infection of adults. J. Infect. Dis 212: 1719–1725. [PubMed: 25977264]

86. Habibi MS, Thwaites RS, Chang M, Jozwik A, Paras A, Kirsebom F, Varese A, Owen A, Cuthbertson L, James P, Tunstall T, Nickle D, Hansel TT, Moffatt MF, Johansson C, Chiu C, and Openshaw PJM. 2020. Neutrophilic inflammation in the respiratory mucosa predisposes to RSV infection. Science 370: eaba9301. [PubMed: 33033192]

87. Huang K, Incognito L, Cheng X, Ulbrandt ND, and Wu H. 2010. Respiratory syncytial virus-neutralizing monoclonal antibodies motavizumab and palivizumab inhibit fusion. J. Virol 84: 8132–8140. [PubMed: 20519399]

88. 1998. Palivizumab, a humanized respiratory syncytial virus monoclonal antibody, reduces hospitalization from respiratory syncytial virus infection in high-risk infants. Pediatrics 102: 531–537.

89. Liljeroos L, Krzyzaniak MA, Helenius A, and Butcher SJ. 2013. Architecture of respiratory syncytial virus revealed by electron cryotomography. Proc. Natl. Acad. Sci. USA 110: 11133–11138. [PubMed: 23776214]

90. Habibi MS, Jozwik A, Makris S, Dunning J, Paras A, DeVincenzo JP, de Haan CA, Wrammert J, Openshaw PJ, Chiu C, and I. Mechanisms of Severe Acute Influenza Consortium. 2015. Impaired antibody-mediated protection and defective IgA B-cell memory in experimental infection of adults

with respiratory syncytial virus. Am. J. Respir. Crit. Care Med 191: 1040–1049. [PubMed: 25730467]

91. Jounai N, Yoshioka M, Tozuka M, Inoue K, Oka T, Miyaji K, Ishida K, Kawai N, Ikematsu H, Kawakami C, Shimizu H, Mori M, Ishii KJ, and Takeshita F. 2017. Age-specific profiles of antibody responses against respiratory syncytial virus infection. EBioMedicine 16: 124–135. [PubMed: 28111238]
92. Walsh EE, and Falsey AR. 2004. Humoral and mucosal immunity in protection from natural respiratory syncytial virus infection in adults. J. Infect. Dis 190: 373–378. [PubMed: 15216475]
93. Alansari K, Toaimah FH, Almatar DH, El Tatawy LA, Davidson BL, and Qusad MIM. 2019. Monoclonal antibody treatment of RSV bronchiolitis in young infants: A randomized trial. Pediatrics 143: e20182308. [PubMed: 30760509]
94. Hogan RJ, Usherwood EJ, Zhong W, Roberts AA, Dutton RW, Harmsen AG, and Woodland DL. 2001. Activated antigen-specific CD8+ T cells persist in the lungs following recovery from respiratory virus infections. J. Immunol 166: 1813–1822. [PubMed: 11160228]
95. Connor LM, Harvie MC, Rich FJ, Quinn KM, Brinkmann V, Le Gros G, and Kirman JR. 2010. A key role for lung-resident memory lymphocytes in protective immune responses after BCG vaccination. Eur. J. Immunol 40: 2482–2492. [PubMed: 20602436]
96. Pizzolla A, Nguyen THO, Smith JM, Brooks AG, Kedzieska K, Heath WR, Reading PC, and Wakim LM. 2017. Resident memory CD8(+) T cells in the upper respiratory tract prevent pulmonary influenza virus infection. Sci. Immunol 2: eaam6970. [PubMed: 28783656]
97. Jorquera PA, Choi Y, Oakley KE, Powell TJ, Boyd JG, Palath N, Haynes LM, Anderson LJ, and Tripp RA. 2013. Nanoparticle vaccines encompassing the respiratory syncytial virus (RSV) G protein CX3C chemokine motif induce robust immunity protecting from challenge and disease. PLoS One 8: e74905. [PubMed: 24040360]
98. Espeseth AS, Cejas PJ, Citron MP, Wang D, DiStefano DJ, Callahan C, Donnell GO, Galli JD, Swoyer R, Touch S, Wen Z, Antonello J, Zhang L, Flynn JA, Cox KS, Freed DC, Vora KA, Bahl K, Latham AH, Smith JS, Gindy ME, Ciaramella G, Hazuda D, Shaw CA, and Bett AJ. 2020. Modified mRNA/lipid nanoparticle-based vaccines expressing respiratory syncytial virus F protein variants are immunogenic and protective in rodent models of RSV infection. NPJ Vaccines 5: 16.
99. Kim KH, Lee YT, Hwang HS, Kwon YM, Kim MC, Ko EJ, Lee JS, Lee Y, and Kang SM. 2015. Virus-like particle vaccine containing the F protein of respiratory syncytial virus confers protection without pulmonary disease by modulating specific subsets of dendritic cells and effector T cells. J. Virol 89: 11692–11705. [PubMed: 26355098]
100. Schwarz B, Morabito KM, Ruckwardt TJ, Patterson DP, Avera J, Miettinen HM, Graham BS, and Douglas T. 2016. Viruslike particles encapsidating respiratory syncytial virus M and M2 proteins induce robust T cell responses. ACS Biomater. Sci. Eng 2: 2324–2332. [PubMed: 29367948]
101. Schmidt ME, Knudson CJ, Hartwig SM, Pewe LL, Meyerholz DK, Langlois RA, Harty JT, and Varga SM. 2018. Memory CD8 T cells mediate severe immunopathology following respiratory syncytial virus infection. PLoS Pathog. 14: e1006810. [PubMed: 29293660]
102. Luangrath MA, Schmidt ME, Hartwig SM, and Varga SM. 2021. Tissue-resident memory T cells in the lungs protect against acute respiratory syncytial virus infection. Immunohorizons 5: 59–69. [PubMed: 33536235]
103. Mapletoft JW, Latimer L, Babiuk LA, and van S Drunen Littel-van den Hurk. 2010. Intranasal immunization of mice with a bovine respiratory syncytial virus vaccine induces superior immunity and protection compared to those by subcutaneous delivery or combinations of intranasal and subcutaneous prime-boost strategies. Clin. Vaccine Immunol 17: 23–35. [PubMed: 19864487]
104. Ichinohe T, Ainai A, Tashiro M, Sata T, and Hasegawa H. 2009. PolyI:polyC12U adjuvant-combined intranasal vaccine protects mice against highly pathogenic H5N1 influenza virus variants. Vaccine 27: 6276–6279. [PubMed: 19840660]
105. McGinnes Cullen L, Schmidt MR, Kenward SA, Woodland RT, and Morrison TG. 2015. Murine immune responses to virus-like particle-associated pre- and postfusion forms of the respiratory syncytial virus F protein. J. Virol 89: 6835–6847. [PubMed: 25903340]

106. Kamphuis T, Stegmann T, Meijerhof T, Wilschut J, and de Haan A. 2013. A virosomal respiratory syncytial virus vaccine adjuvanted with monophosphoryl lipid A provides protection against viral challenge without priming for enhanced disease in cotton rats. Influenza Other Respir. Viruses 7: 1227–1236. [PubMed: 23575113]

107. Fries L, Shinde V, Stoddard JJ, Thomas DN, Kpamegan E, Lu H, Smith G, Hickman SP, Piedra P, and Glenn GM. 2017. Immunogenicity and safety of a respiratory syncytial virus fusion protein (RSV F) nanoparticle vaccine in older adults. Immun. Ageing 14: 8. [PubMed: 28413427]

108. Munoz FM, Swamy GK, Hickman SP, Agrawal S, Piedra PA, Glenn GM, Patel N, August AM, Cho I, and Fries L. 2019. Safety and immunogenicity of a respiratory syncytial virus fusion (F) protein nanoparticle vaccine in healthy third-trimester pregnant women and their infants. J. Infect. Dis 220: 1802–1815. [PubMed: 31402384]

109. Kamphuis T, Shafique M, Meijerhof T, Stegmann T, Wilschut J, and de Haan A. 2013. Efficacy and safety of an intranasal virosomal respiratory syncytial virus vaccine adjuvanted with monophosphoryl lipid A in mice and cotton rats. Vaccine 31: 2169–2176. [PubMed: 23499594]

110. Gu H, Li T, Han L, Zhu P, Zhang P, Zhang S, Sun S, Duan Y, Xing L, Zhao Z, Lai C, Wen B, Wang X, and Yang P. 2015. Protection conferred by virus-like particle vaccines against respiratory syncytial virus infection in mice by intranasal vaccination. Hum. Vaccin. Immunother 11: 1057–1064. [PubMed: 25933187]

111. Lipford GB, Sparwasser T, Zimmermann S, Heeg K, and Wagner H. 2000. CpG-DNA-mediated transient lymphadenopathy is associated with a state of Th1 predisposition to antigen-driven responses. J. Immunol 165: 1228–1235. [PubMed: 10903720]

112. Vogel AJ, and Brown DM. 2015. Single-dose CpG immunization protects against a heterosubtypic challenge and generates antigen-specific memory T cells. Front. Immunol 6: 327. [PubMed: 26161083]

113. Grun JL, and Maurer PH. 1989. Different T helper cell subsets elicited in mice utilizing two different adjuvant vehicles: the role of endogenous interleukin 1 in proliferative responses. Cell Immunol. 121: 134–145. [PubMed: 2524278]

114. Marrack P, McKee AS, and Munks MW. 2009. Towards an understanding of the adjuvant action of aluminium. Nat. Rev. Immunol 9: 287–293. [PubMed: 19247370]

115. Petersen LK, Xue L, Wannemuehler MJ, Rajan K, and Narasimhan B. 2009. The simultaneous effect of polymer chemistry and device geometry on the in vitro activation of murine dendritic cells. Biomaterials 30: 5131–5142. [PubMed: 19539989]

**Key points**

- RSVNanoVax enhances viral clearance in both inbred and outbred mice.
- RSVNanoVax induces systemic and local F-directed antibody responses.
- Vaccination with RSVNanoVax induces tissue-resident memory CD4 and CD8 T cells.

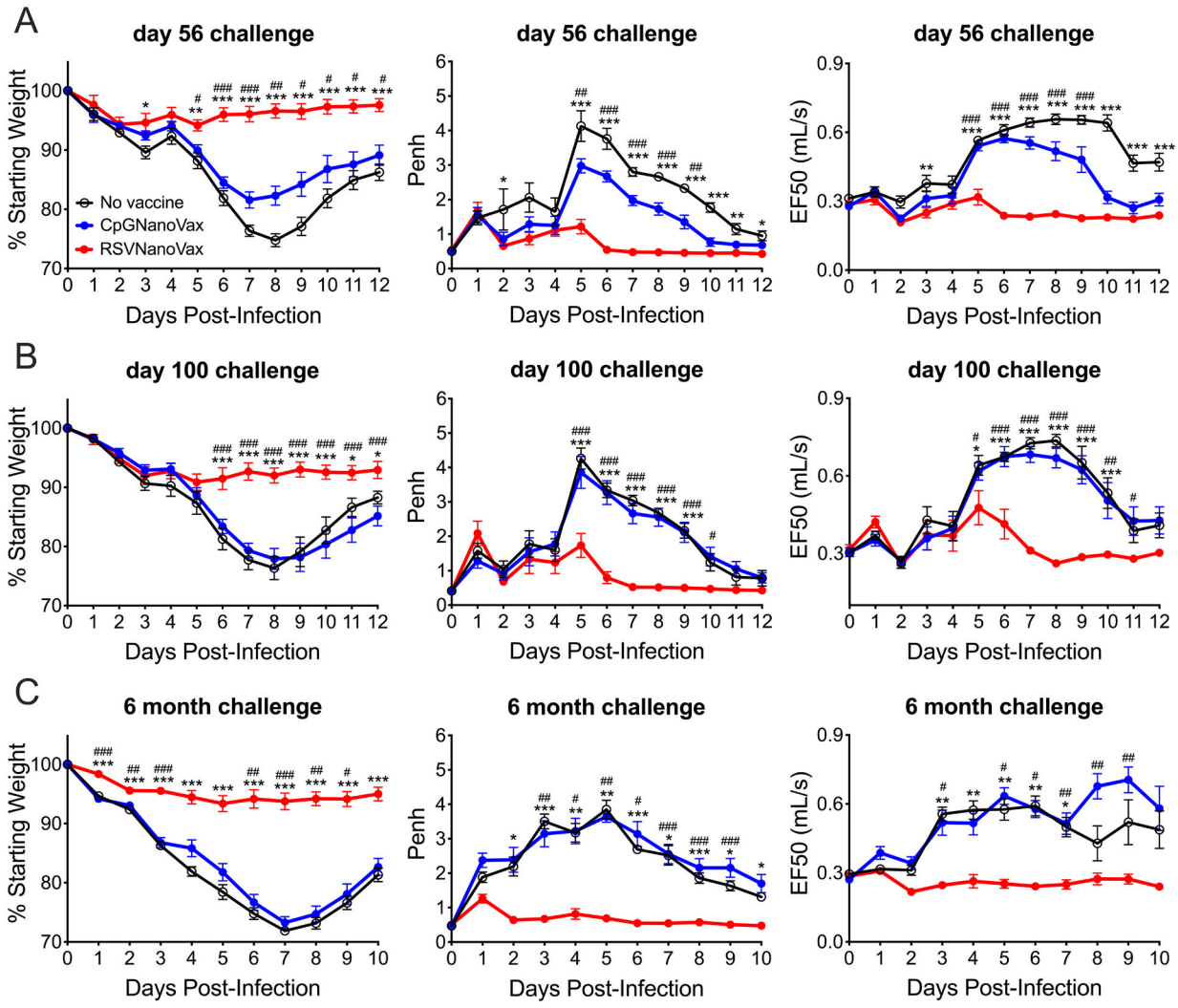


**Figure 1. Prime-boost vaccination with RSVNanoVax protects against RSV-induced weight loss and pulmonary dysfunction.**

BALB/c mice were primed i.n. on day 0 and boosted with 500 μg on day 28. All mice were challenged with $4.8 \times 10^6$ PFU RSV-A2 on day 56 **(A)**, day 100 **(B)**, or 6 months **(C)** post-prime and assessed for weight loss and pulmonary dysfunction as measured by baseline changes in Penh and EF50. Asterisks represent significance between no vaccine and RSVNanoVax and pound symbols represent significance between CpGNanoVax and RSVNanoVax as determined by 2-way ANOVA with a Dunnett's post hoc test. $*/\#$ $p<0.05$, $**/\#\#$ $p<0.01$, $***/\#\#\#$ $p<0.001$. No vaccine mice were administered PBS i.n. at both the prime and boost. Data represent mean ± SEM of 2–3 independent experiments ($n$=8–12).

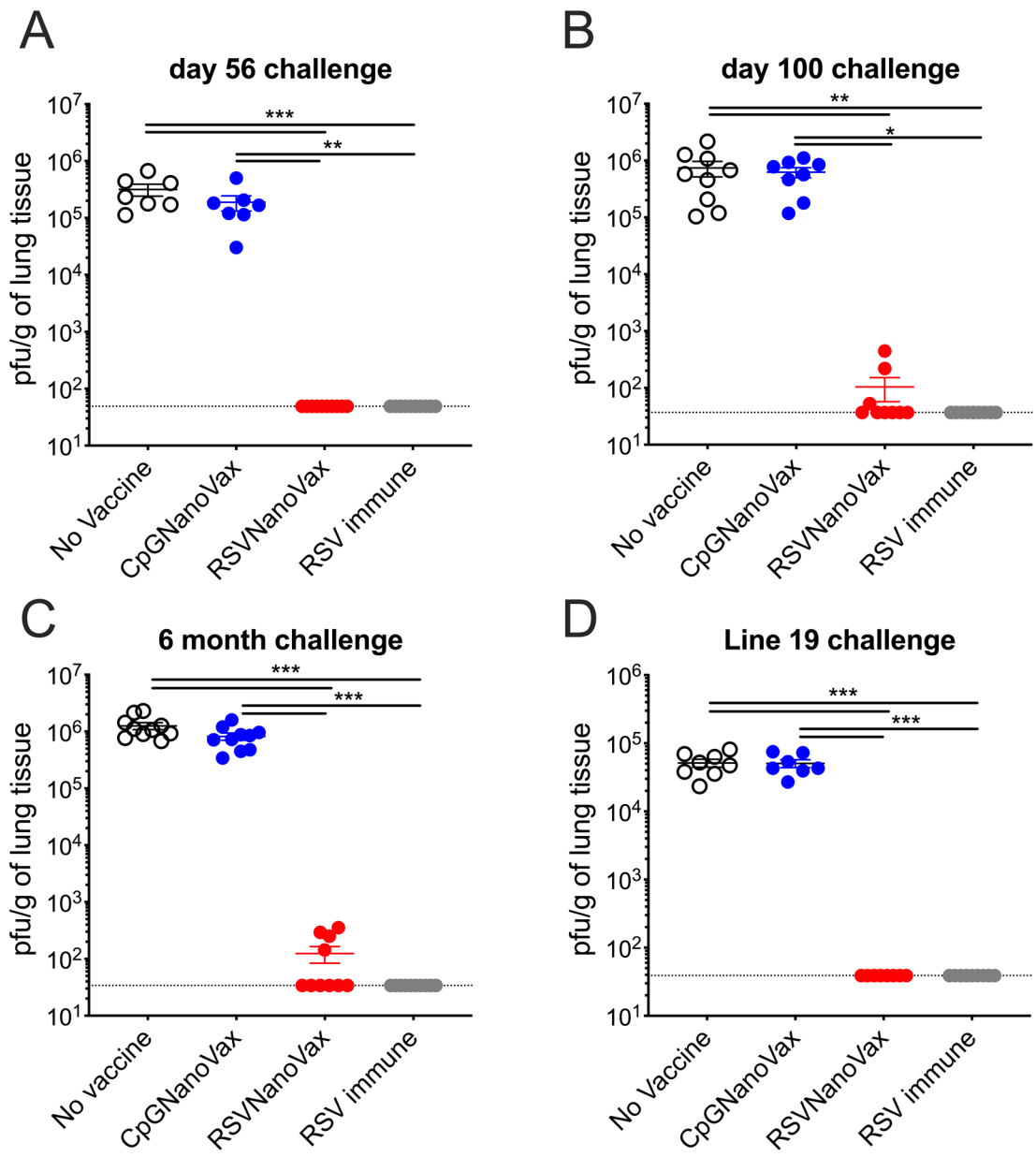


**Figure 2. Prime-boost RSVNanoVax immunization reduces infectious RSV particles in the lungs.**

BALB/c mice were primed i.n. on day 0 and boosted with 500μg on day 28. On day 56 **(A)**, day 100 **(B)**, or 6 months **(C)** post-prime mice were challenged with $4.8 \times 10^6$ PFU RSV-A2 and infectious viral pfu were quantified in the lung on day 4 post-infection. **(D)** Vaccinated mice were challenged with $1.1 \times 10^6$ PFU RSV line 19 on day 56 and infectious viral pfu were quantified in the lung on day 4 post-infection. Statistical significance was determined by one-way ANOVA with a Tukey's post hoc test. *$p$<0.05, **$p$<0.01, ***$p$<0.001. No vaccine mice were administered PBS i.n. at both the prime and boost. RSV immune mice received $4.8 \times 10^6$ PFU RSV-A2 at the prime and PBS i.n. at the boost. Data represent mean ± SEM of 2 independent experiments ($n$=7–10). The horizontal dashed line represents the limit of detection.

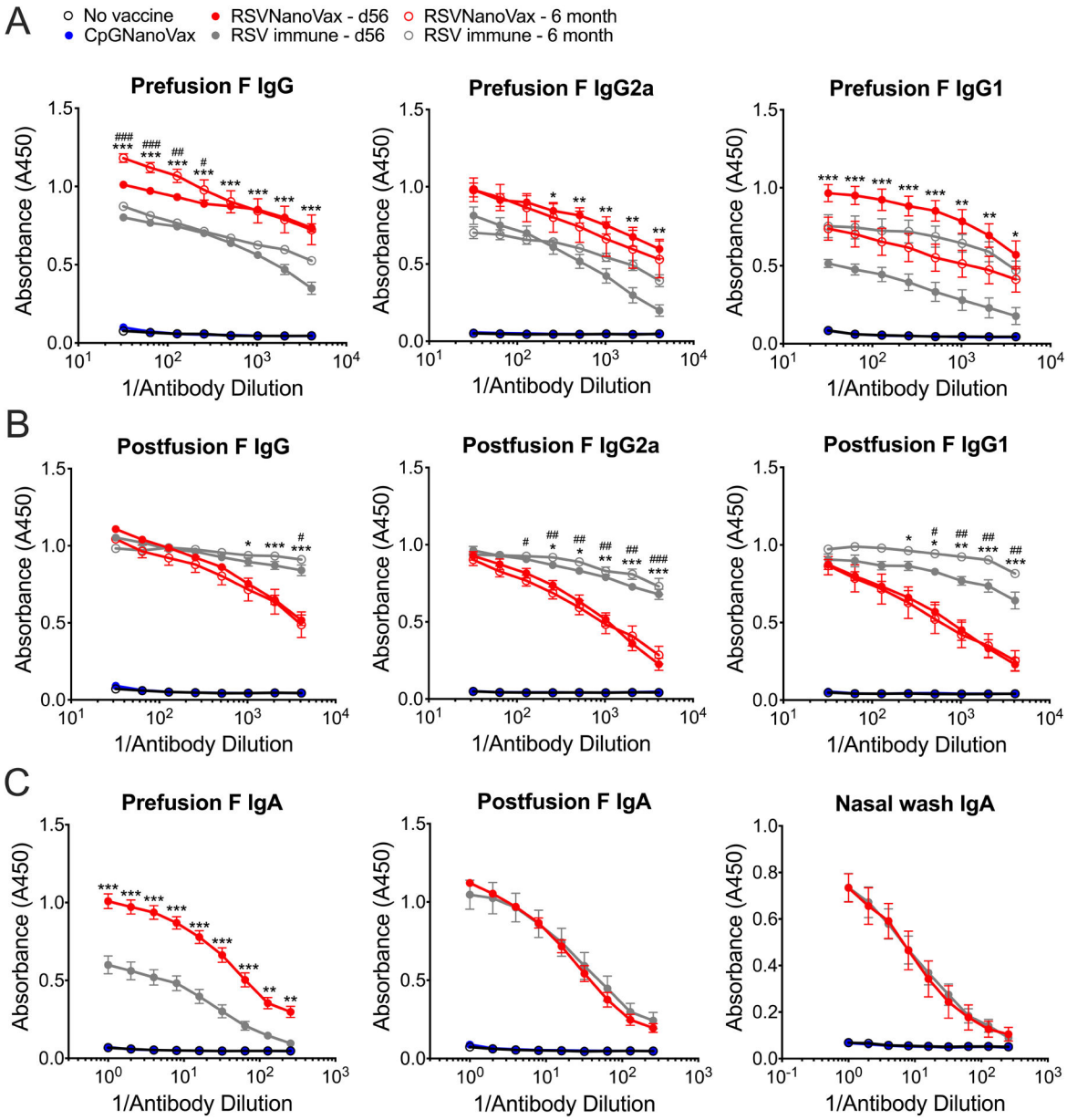


**Figure 3. Prime-boost RSVNanoVax vaccination induces RSV-specific systemic and local antibody responses.**

Serum was collected from WT mice that received a prime and boost of the indicated nanoparticle formulation, naïve mice, or RSV immune mice that received $4.8 \times 10^6$ PFU RSV-A2 56 days or 6 months prior. **(A)** PreF or **(B)** postF-directed total IgG, IgG1, or IgG2a was measured by antibody ELISA. **(C)** F-specific IgA was measured in either whole lung homogenates (preF and postF) or nasal wash fluid (preF only) on day 56 by antibody ELISA. Statistical significance was determined by a 2-way ANOVA with a Dunnett's post hoc test. Asterisks represent significance between RSVNanoVax d56 and RSV immune d56 and pound symbols represent significance between RSVNanoVax 6 month and RSV immune 6 month. $*/\#$ $p<0.05$, $**/\#\#$ $p<0.01$, $***/\#\#\#$ $p<0.001$. Data represent mean ± SEM of 2 independent experiments ($n$=8–10).

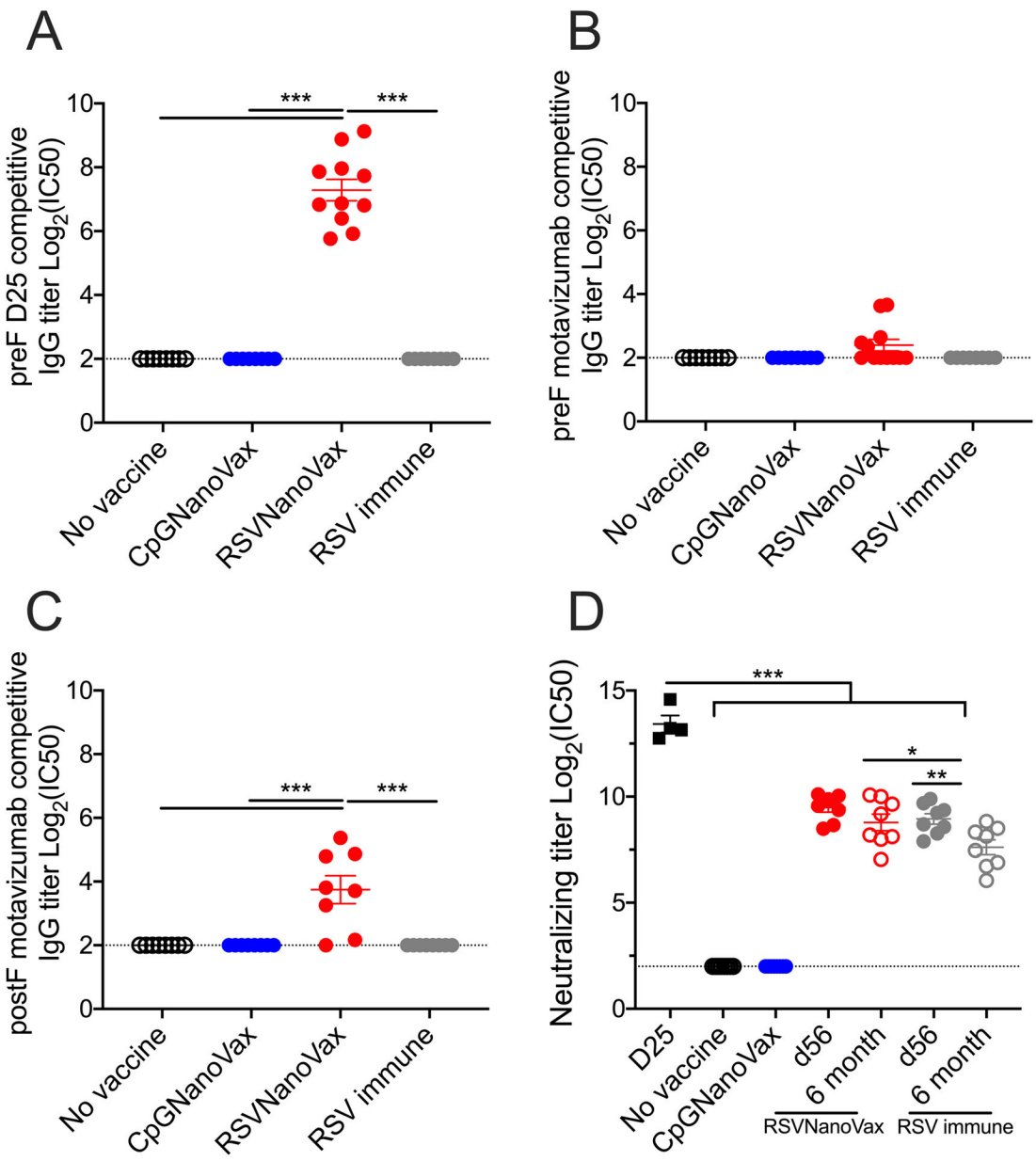


**Figure 4. Prime-boost RSVNanoVax vaccination induces RSV-specific serum antibodies with neutralizing capability.**

Serum was collected from WT mice that received a prime and boost of the indicated nanoparticle formulation, naïve mice, or RSV immune mice that received $4.8 \times 10^6$ PFU RSV-A2 56 days or 6 months prior. **(A-C)** RSVNanoVax RSV F site-specific competitive binding was determined by competition antibody ELISA. Competition with **(A)** D25 or **(B)** motavizumab for binding to preF or competition with **(C)** motavizumab for binding to postF. Competitive titers are expressed as log2 of the serum dilution that resulted in 50% inhibition of D25 or motavizumab monoclonal antibody binding to the RSV F protein. **(D)** Neutralizing capacity of serum antibodies was determined by RSV-A2 plaque reduction on Vero cells. Neutralizing titers are expressed as log2 of the serum dilution that resulted in 50% inhibition of viral plaques. Statistical significance was determined by a one-way

ANOVA with a Tukey's post hoc test. *$p$<0.05, **$p$<0.01, ***$p$<0.001. Data represent mean ± SEM of 2 independent experiments ($n$=8–11). The horizontal dashed line represents the limit of detection.

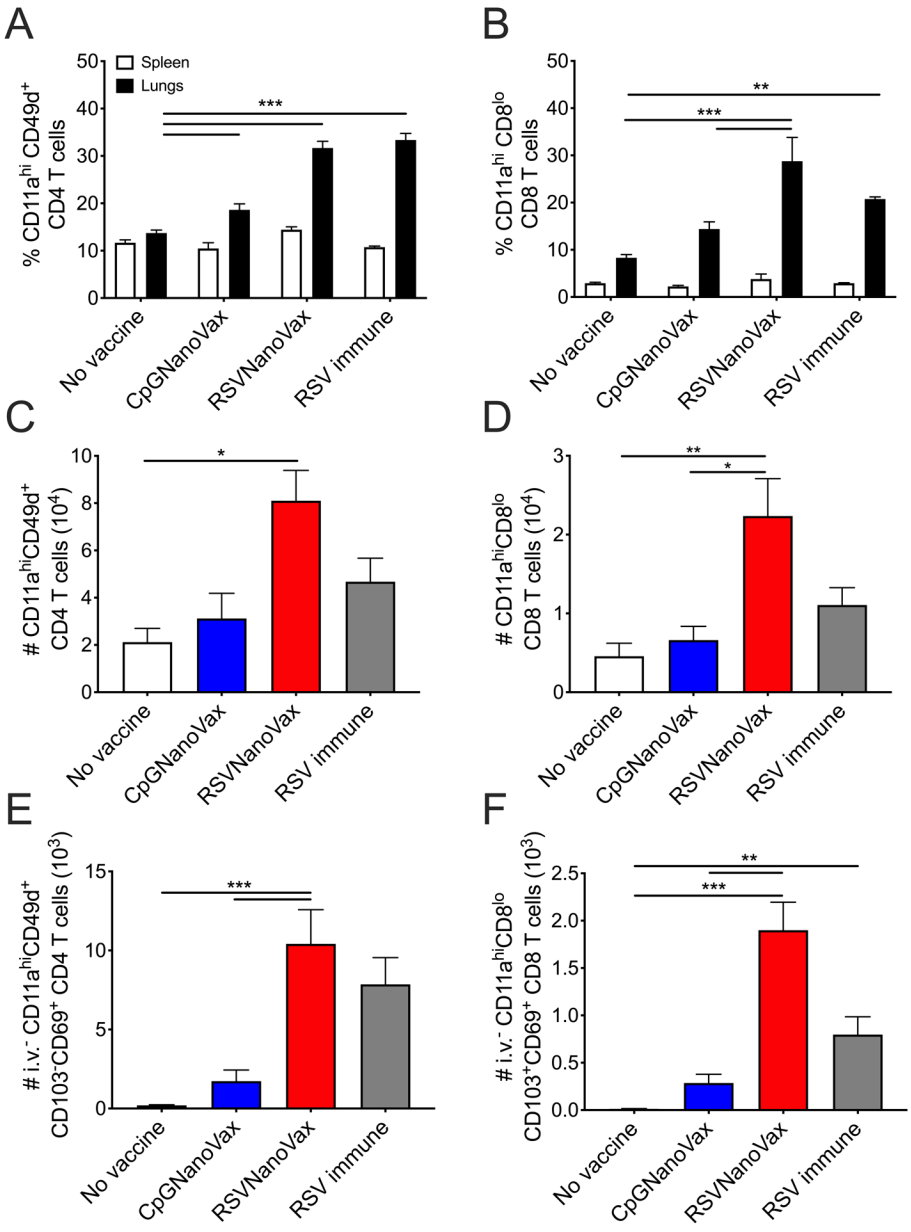


**Figure 5. Antigen-experienced tissue-resident memory CD4 and CD8 T cells are induced by prime-boost RSVNanoVax immunization.**

BALB/c mice were primed with 500 μg of the indicated nanoparticle formulation i.n. on day 0, and boosted with 500 μg i.n. on day 28. No vaccine mice were administered PBS i.n. on both prime and boost days. RSV immune mice received $4.8 \times 10^6$ PFU RSV-A2 i.n. at the prime and PBS i.n. at the boost. Lungs and spleens were harvested on day 42 and analyzed by flow cytometry. Frequency of **(A)** antigen-experienced ($CD11a^{hi}CD49d^{+}$) CD4 T cells and (**B**) antigen-experienced ($CD11a^{hi}CD8^{lo}$) CD8 T cells. Total number of antigen-experienced **(C)** CD4 T cells and **(D)** CD8 T cells in the lung. Number of antigen-experienced CD45 intravascular antibody negative ($i.v.^{-}$) **(E)** $CD103^{-}CD69^{+}$ CD4 T cells and **(F)** $CD103^{+}CD69^{+}$ CD8 T cells. Statistical significance was determined by (A and B) 2-way ANOVA with a Tukey's post hoc test or (C-F) one-way ANOVA with a Tukey's post

hoc test. *$p$<0.05, **$p$<0.01, ***$p$<0.001. Data represent mean ± SEM of 2 independent experiments ($n$=8).

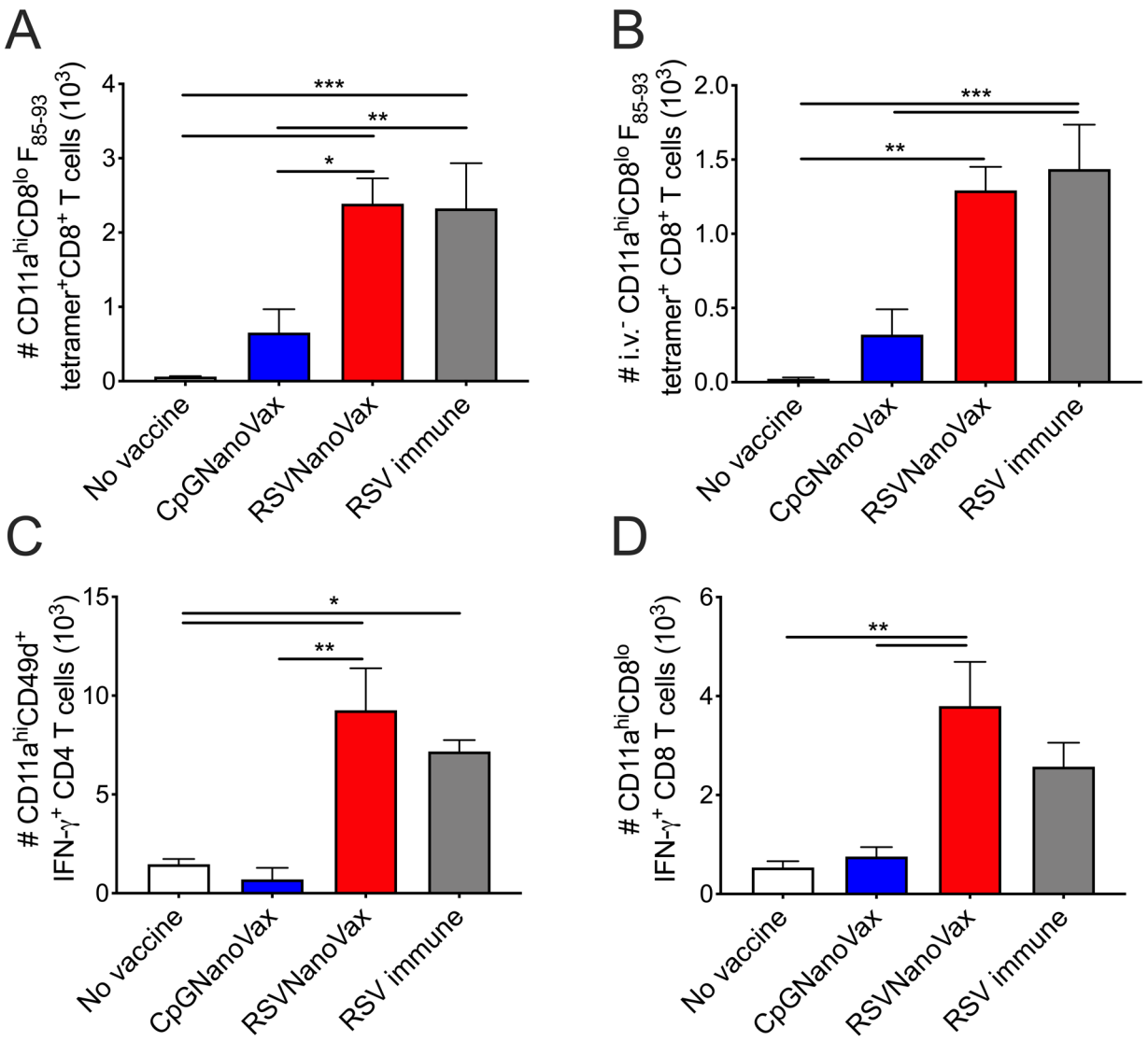


**Figure 6. Prime-boost RSVNanoVax immunization induces RSV-specific functional CD4 and CD8 T cells in the lungs.**

BALB/c mice were primed with 500 μg of the indicated nanoparticle formulation i.n. on day 0, and boosted with 500 μg i.n. on day 28. No vaccine mice were administered PBS i.n. on both prime and boost days. RSV immune mice received $4.8 \times 10^6$ PFU RSV-A2 i.n. at the prime and PBS i.n. at the boost. Lungs were harvested on day 42 and analyzed by flow cytometry. Number of **(A)** antigen-experienced $F_{85–93}$ tetramer$^+$ CD8 T cells and **(B)** i.v.$^-$ antigen-experienced $F_{85–93}$ tetramer$^+$ CD8 T cells. Number of antigen-experienced IFN-$\gamma^+$ **(C)** CD4 and **(D)** CD8 T cells following stimulation with PMA and ionomycin. Statistical significance was determined by one-way ANOVA (A-D) with a Tukey's post hoc test. *$p$<0.05, **$p$<0.01, ***$p$<0.001. Data represent mean ± SEM of 2 independent experiments ($n$=8).

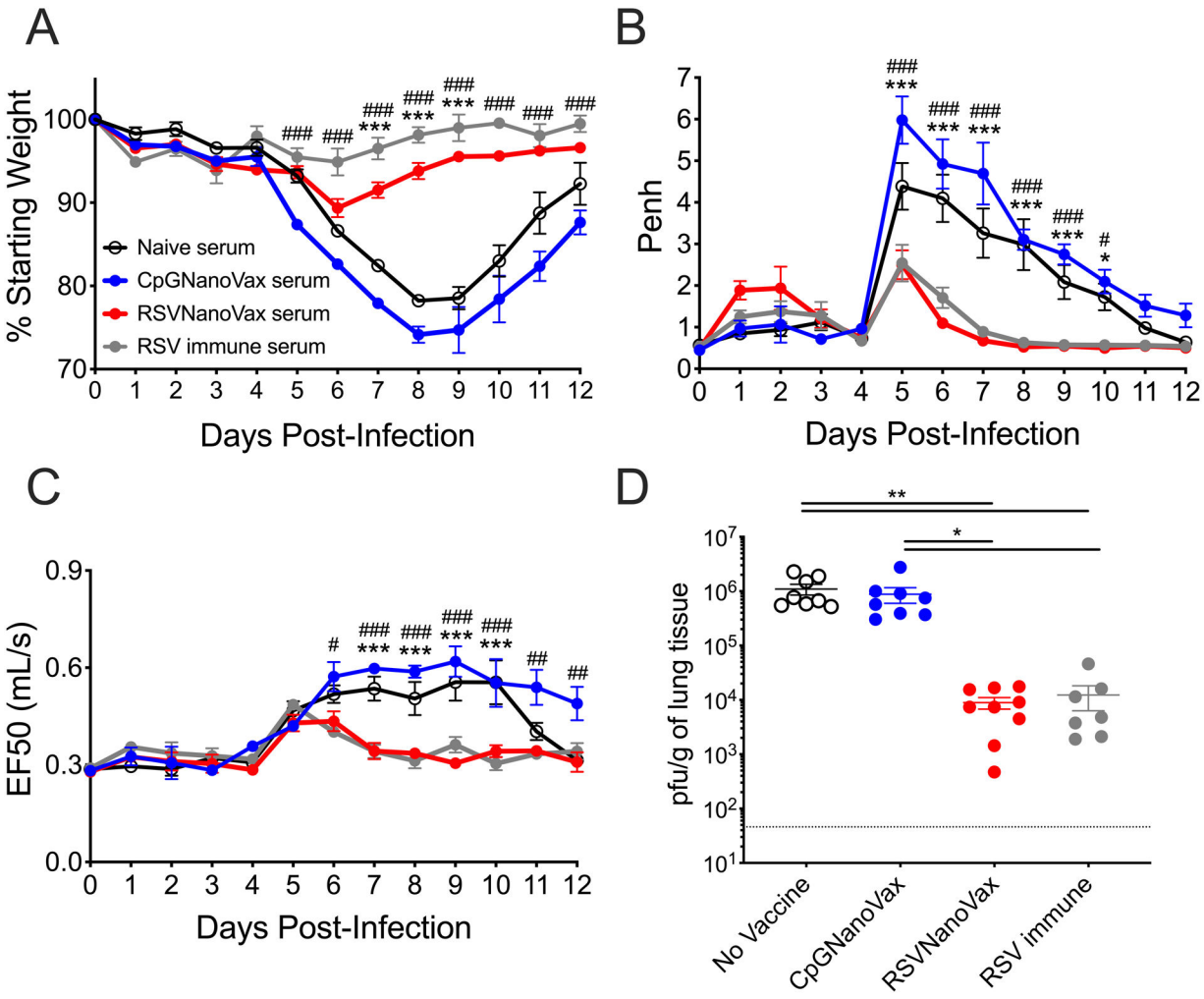


**Figure 7. Protection afforded by RSVNanoVax is partially mediated by systemic antibodies.**

Serum was collected on day 56 from WT donor mice that received a prime and boost of the indicated nanoparticle formulation, naïve mice, or RSV immune mice that received 4.8 × $10^6$ PFU RSV-A2 56 days prior. Recipient BALB/c mice were administered 200 μL serum i.p.. At 24 hours all mice were challenged with 4.8 × $10^6$ PFU RSV-A2 i.n. **(A-C)** Groups were monitored daily for **(A)** weight loss, **(B)** Penh, and **(C)** EF50. Asterisks represent significance between no vaccine and RSVNanoVax and pound symbols represent significance between CpGNanoVax and RSVNanoVax as determined by 2-way ANOVA with a Dunnett's post hoc test. **(D)** Infectious viral PFU were quantified in the lung on day 4 post-infection by plaque assay. Statistical significance was determined by one-way ANOVA with a Tukey's post hoc test. $*^{/\#}$ $p<0.05$, $**^{/\#\#}$ $p<0.01$, $***^{/\#\#\#}$ $p<0.001$. Data represent mean ± SEM of 2 independent experiments ($n=9$). The horizontal dashed line represents the limit of detection.

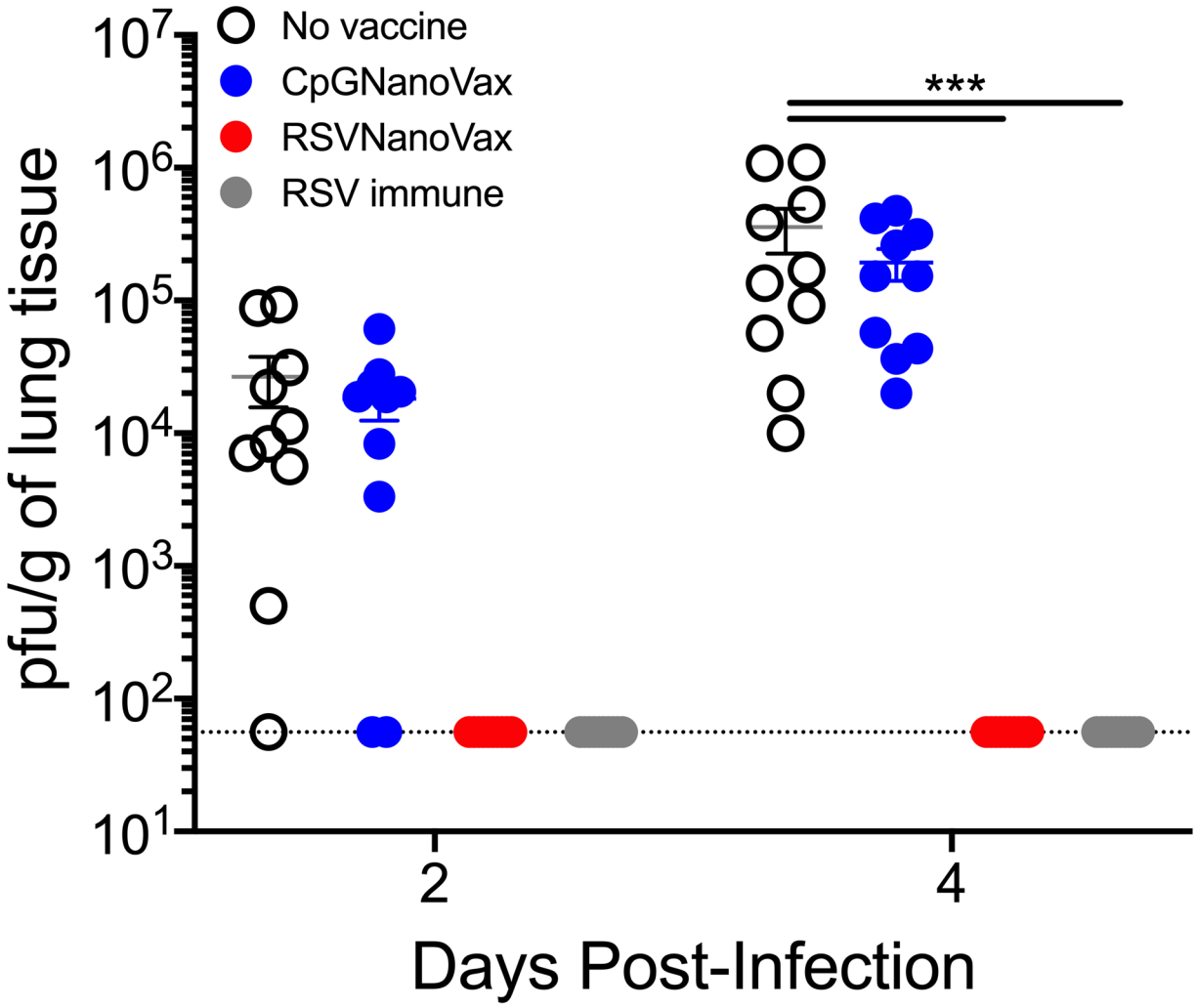


**Figure 8. Prime-boost RSVNanoVax vaccination mediates viral clearance in an outbred population.**

Swiss Webster mice were primed with 500 μg of the indicated nanoparticle formulation i.n. on day 0, and boosted with 500 μg i.n. on day 28. No vaccine mice were administered PBS i.n. at both the prime and boost. RSV immune mice received $4.8 \times 10^6$ PFU RSV-A2 i.n. at the prime and PBS i.n. at the boost. All mice were challenged with $4.8 \times 10^6$ PFU RSV-A2 on day 56. Infectious viral PFU were quantified in the lung on day 2 or 4 post-infection by plaque assay. Statistical significance was determined by 2-way ANOVA with a Tukey's post hoc test. ***$p<0.001$. Data represent mean ± SEM of 2 independent experiments ($n$=8–10). The horizontal dashed line represents the limit of detection.

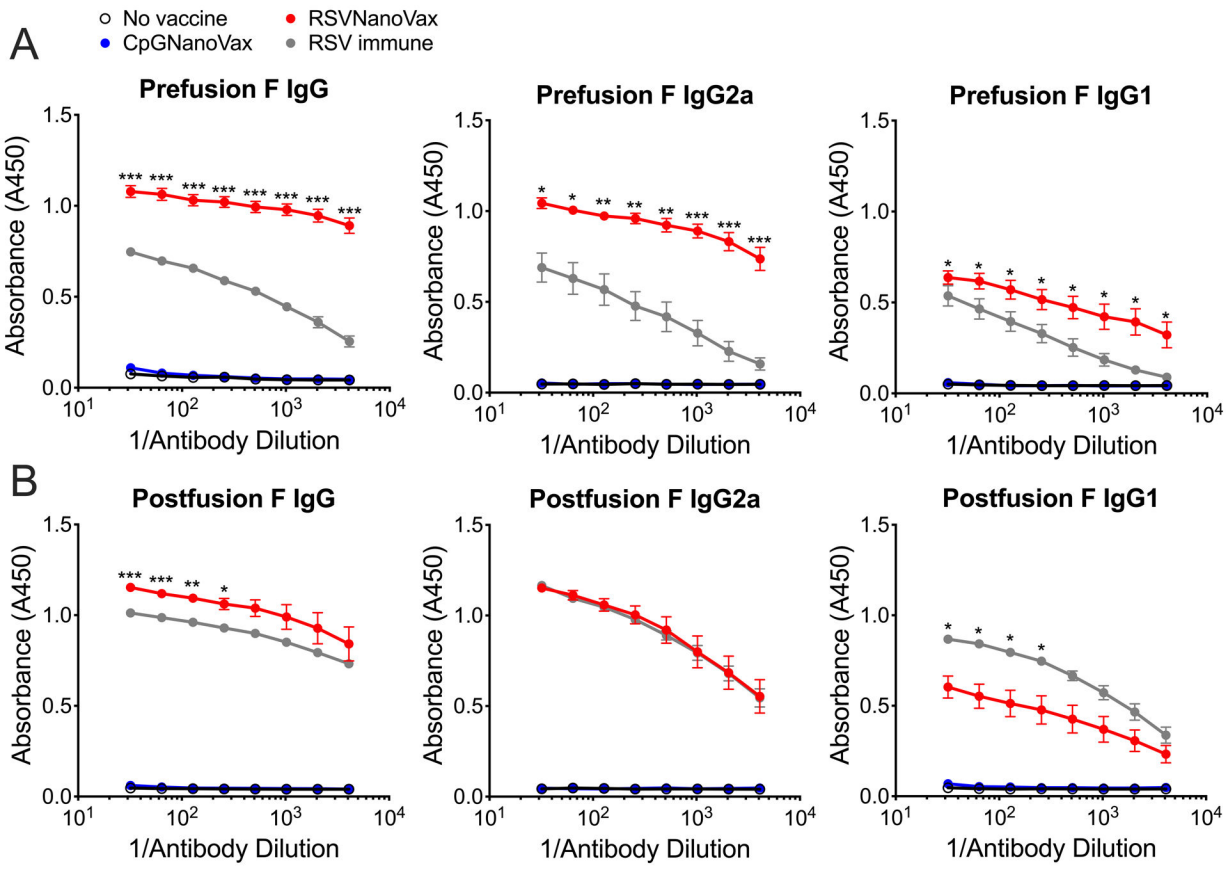


**Figure 9. Prime-boost RSVNanoVax vaccination induces systemic RSV-specific antibodies in an outbred population.**

Serum was collected from Swiss Webster mice that received a prime and boost of the indicated nanoparticle formulation, naïve mice, or RSV immune mice that received 4.8 × $10^6$ PFU RSV-A2 56 days or 6 months prior. **(A)** PreF or **(B)** postF-directed total IgG, IgG1, or IgG2a antibodies were measured by antibody ELISA. Statistical significance was determined by 2-way ANOVA with a Tukey's post hoc test. Asterisks represent significance between RSVNanoVax and RSV immune. *$p$<0.05, **$p$<0.01, ***$p$<0.001. Data represent mean ± SEM of 2 independent experiments ($n$=8–10).